

Review

Power management and effective energy storage of pulsed output from triboelectric nanogenerator



Xiaoliang Cheng^a, Wei Tang^b, Yu Song^a, Haotian Chen^a, Haixia Zhang^{a,*}, Zhong Lin Wang^{b,c,**}

^a National Key Laboratory of Nano/Micro Fabrication Technology, Peking University, 100871, Beijing, China

^b Beijing Institute of Nanoenergy and Nanosystems Chinese Academy of Sciences, Beijing, 100083, China

^c School of Materials Science and Engineering, Georgia Institute of Technology, Atlanta, Ga, 30062, USA

ARTICLE INFO

Keywords

Triboelectric nanogenerator

Power management

Energy storage

ABSTRACT

Triboelectric nanogenerator (TENG) harvesting living environmental energy has been demonstrated to be a potential energy source for internet of things, for its unique properties, such as high-output performance, clean, sustainability, low-cost etc., which have resulted in an explosive growth of related research in the past several years. However, due to the unique features of electrical output signals of TENGs like the pulsed output with random amplitude and frequency, ultra-high voltages and impedance, the electrical power generated by TENGs is hard to be delivered to the load efficiently or stored directly by the classical power management methods. Meanwhile, the mechanical energy from the environment is time dependent, unstable and sometime unpredictable, but the power required to drive electronics is regulated with a fixed input voltage and power. So it is important to store the generated energy in a battery or capacitor, so that it can be used to power a device sustainably. Fortunately, both the power management and energy storage for TENG have obtained significantly progress recently. Here, this paper reviews the progress made in power management and storage, including theoretical development, charge boosting, buck converting, energy storage, and the new enabled applications, aiming at building a self-charging power unit (SCPU) that can be a standard power package for sustainable operation of an electronic device. Finally, we will give an outlook for future development of applying SCPU for internet of things.

1. Introduction

There are urgent demands for sustainable and stable power source caused by the rapid progress in wearable electronics [1,2], internet of things (IOTs) [3], and implantable electronics devices [4] made in recent years. Batteries and capacitors are usually employed to supply power for these devices [5–7], which have to be frequently charged or replaced due to their limited capacity and big volume, thus turning into unpractical and unfavorable. Harvesting energy from the mechanical energy of ambient environment or biomechanical energy of human motion for sustainable working is one of the most promising strategies to deal with such issues [8–10]. In the last years, the triboelectric nanogenerator (TENG) is emerging as a potential energy-harvesting method [10–13], which has the advantages of high performance [14–19], light weight [20–22], simple structure [16,23–28], cost-effective [29–31] etc. Many kinds of mechanical energies from ocean wave [32–34], wind [35–37], human motions [38–42] and even

heartbeat [43] have been successfully converted to electricity via TENG.

However, as the existence of intrinsic capacitance, TENG has a large internal impedance of typically in several Mega ohms' level [11,44]. So TENG usually has a large voltage of hundreds of volts and small current in μA level. Since the impedances of electronic device and energy storage unit are relatively low, the energy transfer efficiency would be very low when directly using TENG as a power source [44,45]. Meanwhile, mechanical energy in environment usually is very irregular, making that the output from TENG has pulsed waveform with random amplitude and frequency, and the classical power management methods are thus not effective here. Therefore, a proper power management design is of great urgency for TENG to supply power for electronic devices and charge energy storage unit. Fortunately, significantly improvement and exciting results have been achieved recently. On the basis of analyzing the theoretical model, researchers have put forward a series solutions and strategies for improving the

* Corresponding author.

** Corresponding author. Beijing Institute of Nanoenergy and Nanosystems Chinese Academy of Sciences, Beijing, 100083, China.

E-mail address: hxzhang@pku.edu.cn (H. Zhang).

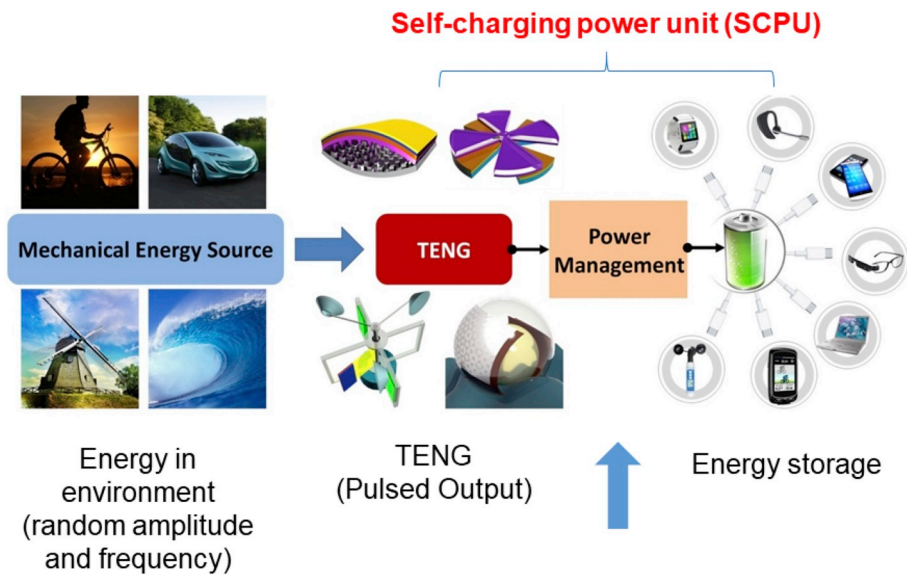


Fig. 1. The concept of self-charging power unit (SCPU) by integrating a TENG, power management circuit and energy storage unit. Reproduced with permission. Reproduced with permission [62]. 2015, Nature.

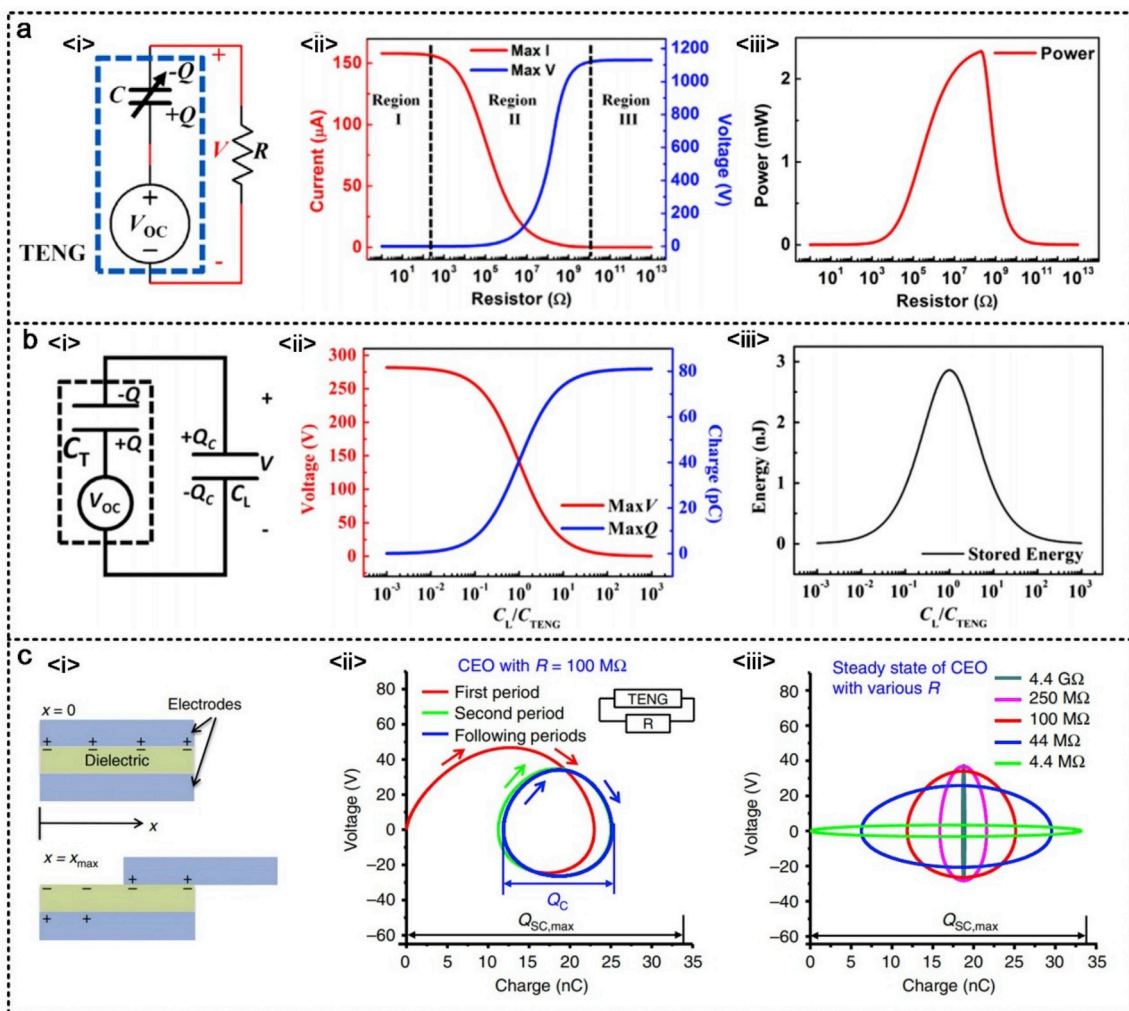


Fig. 2. Theoretical analysis of TENG. (a) The equivalent circuit of the whole system when TENG is connected with resistance loads, and the values of the voltage, current and power on different loads of typical TENGs. (b) The equivalent circuit of the whole system when TENG is connected with capacitive load, and the values of voltage, storage charges, and energy charged to different capacitance in single cycle by typical TENGs. Reproduced with permission [44]. 2015, Elsevier. (c) Schematic diagram of the LS-mode TENG and plots of cycles for energy output with various load resistances. Reproduced with permission [50]. 2015, Nature.

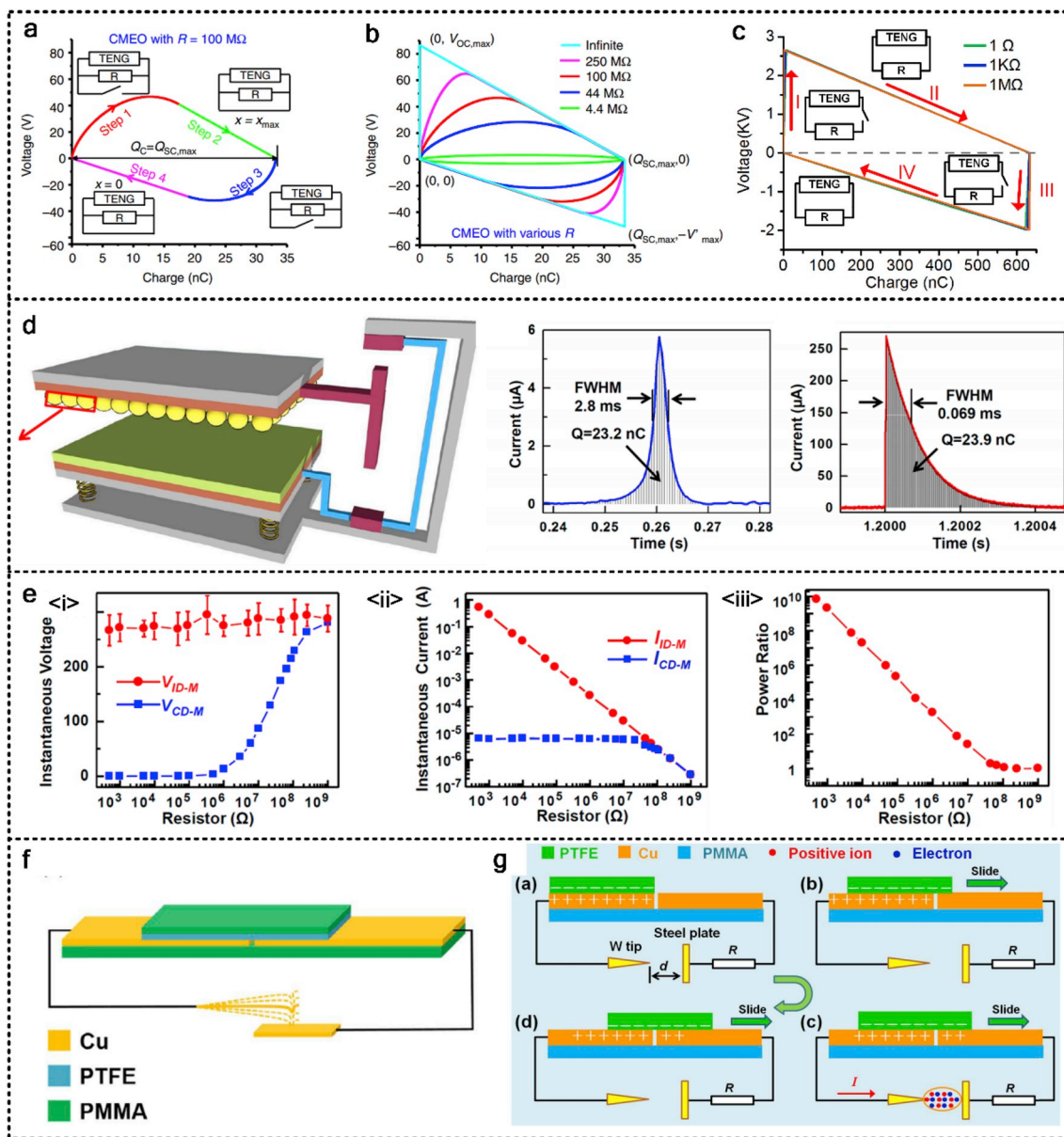


Fig. 3. Cycles for maximized energy output (CMEO) of TENG. (a) The CMEO with load resistance $R = 100 \text{ M}\Omega$, with the maximum total cycling charge $Q_C = Q_{SC,max}$ using a parallel switch. (b) The CMEO with various load resistances. Reproduced with permission [50]. 2015, Nature. (c) The CMEO with 1Ω , 10Ω and $100 \text{ M}\Omega$ load resistance using a serial switch. Reproduced with permission [52]. 2017, Elsevier. (d) Diagram of the instantaneous discharging TENG and comparison of a single current peak of the normal TENG and discharging TENG. (e) Comparisons of instantaneous voltage, instantaneous current of normal TENG and discharging TENG. Reproduced with permission [51]. 2013, ACS. (f) The structure diagram of the TENG with an electrostatic vibrator switch. Reproduced with permission [109]. 2018, Elsevier. (g) The diagram of the working mechanism of the TENG with a self-powered air discharge switch. Reproduced with permission [98]. 2018, Elsevier.

efficiencies of energy transferring and power management module (PMM) [44,46–50]. Generally, these achievements can be summarized as charge boosting [50–57] and buck converting [52,58–64] for TENG. Charge boosting means extracting more charge from TENG to realize higher performance, while buck converting is to transform the high voltage and low current into low voltage and high current.

Besides, without energy storage, the renewable electricity generation from TENG would be less viable. For example, when the mechanical energy doesn't exist or the average power isn't sufficient for the working of commercial electronics, the power supply would become invalid. For sustainable power sources, TENG and energy storage device need to be combined complementarily [65]. Compared with traditional energy source, TENG has the great advantage of flexibility and bendability. The use of traditional rigid battery packs or bulk capacitors as a

power source remains a bottleneck for the development of wearable electronics using TENG as a power source. Recent researches on flexible and bendable batteries and supercapacitors (SCs) exhibit the possibility of overcoming these problems [66–77]. Meanwhile, some works proposed a novel method to integrate TENG and power storage unit, forming a self-charging power unit (SCPU) [78–91]. The integrated solutions can provide more opportunities for sustainable and maintenance-free applications.

In this review, we primarily focus on the functions and developments of power management and energy storage of pulsed output from TENG (Fig. 1) [62], aiming at building a SCPU. We will first have a concise discussion on fundamentals of the electrical model of the TENG, which will be followed by an introduction of the behavior using resistive and capacitive loads and a useful tools of plot of built-up voltage

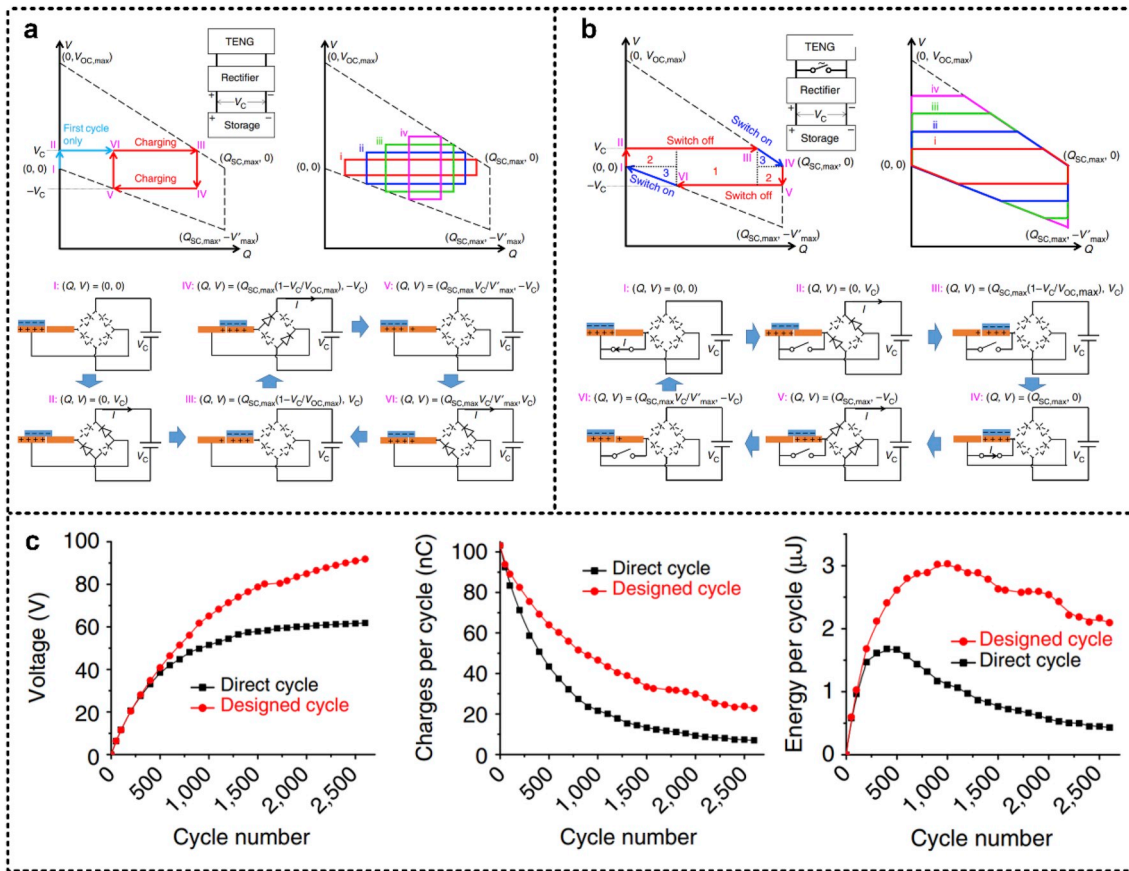


Fig. 4. Effective energy storage from TENG. (a) The V-Q plot and the physical process of the direct charging cycle. (b) The V-Q plot and the physical process of the rationally designed charging cycle. (c) Quantitative comparisons between the charging cycles. Reproduced with permission [55]. 2016, Nature.

V against the transferred charges Q (V-Q plot) for analyzing the electric performance of TENG. Then we will have detailed elaboration on the recent progress on charge boosting, buck converting and energy storage for TENG. Some representative applications using power management module and energy storage unit would be reviewed afterwards. Finally, we would also like to present our thoughts about challenges and prospects of this field in the end.

2. Theoretical analysis

For properly managing the electric output of TENG, its theoretical model should be well understood firstly. In this section, we will discuss basic electric model of TENG. Then, the signal characteristics using resistive and capacitive load will be introduced on the base of this model for readers to understand the urgency of designing a power management module suitable for TENG. Finally, by using the V-Q plot, the cycles for energy output of TENG will be presented.

2.1. Theoretical model of TENG

Usually, TENGs can be divided into four basic modes that are vertical contact-separation mode [92], in-plane sliding mode [92], single electrode mode [93], and free-standing mode [94]. According to previous theoretical works about TENG, the basic working mechanism of TENGs is a conjugation of contact electrification and electrostatic induction [44,46,48]. Fundamentally TENG will have inherent capacitive behavior, since the intrinsic device based on electrostatics is a capacitor [12,20,44,45,47–49,95,96]. For any TENGs, the governing equation

can be given by Refs. [44,47–49].

$$V = -\frac{1}{C(x)}Q + V_{OC}(x) \quad (1)$$

Where V is the total voltage difference between the two electrodes, C and Q represent the capacitance between the two electrodes and the already transferred the charges, V_{OC} is the open circuit voltage between the two electrodes.

From this governing equation, the lumped equivalent circuit model can be derived and represented by a serial connection of an ideal voltage source and a capacitor. It can be noted that the inherent impedance of TENG mainly comes from its inherent capacitance. This lead to an internal high impedance from the small inherent capacitance [44].

2.2. Resistive load characteristics of TENG

When a resistive load R is connected with a TENG, the equivalent circuit is plotted in Fig. 2(a) [44,48]. Utilizing Kirchhoff's law, the governing equation can be determined by

$$R \frac{dQ}{dt} = -\frac{1}{C}Q + V_{OC} \quad (2)$$

The voltages, currents and powers on varying loads of typical TENGs are shown in Fig. 2(a). The working of the TENG could be regarded as three operation regions [44].

Region I, in which the resistance is low (0.1–1000 Ω), the peak value of current has dropped little from the SC state, while the maximum voltage is nearly proportional to the outer resistor.

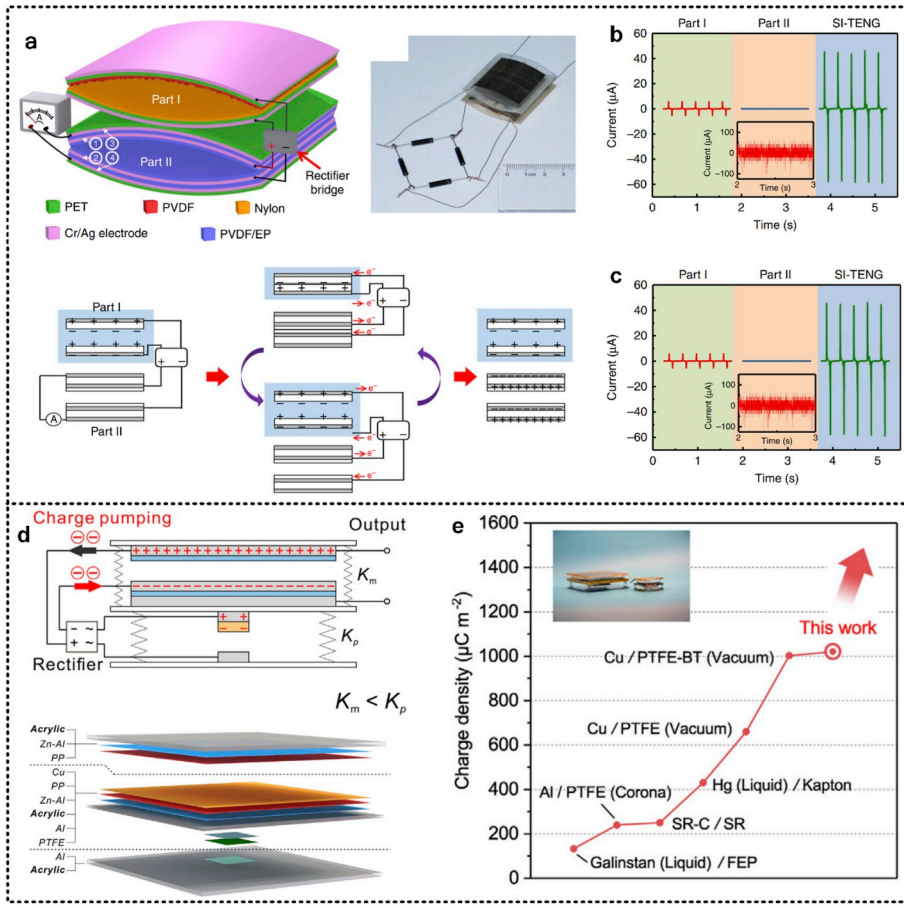


Fig. 5. Charge pump for TENG. (a) Design, structure, and working mechanism of the self-improving TENG. (b–c) The output current and the transferred charge density, respectively, of part I (left lines), part II (middle lines), and the self-improving TENG (SI-TENG) (right lines). Reproduced with permission [54]. 2018, Nature. (d) Schematic structure of the integrated device as a self-charge-pumping (SCP) TENG and the explosive view of the structure and materials of the as-fabricated SCP-TENG. (e) Ultra-high charge density realized in ambient conditions by their work. Reproduced with permission [53]. 2018, Elsevier.

Region II, the maximum current decreases with the resistance while the voltage behaves an opposite trend, and the TENG obtains its maximum output power.

Region III, when the resistor is larger than 1 GΩ, the maximum voltage saturates at V_{OC} .

From the above analyses, we can conclude that the equivalent resistance of TENG are very large (i.e. in Mega ohms' level) since the presence of the inherent resistance of TENG. Therefore, the delivered power would be very small when directly powering a traditional electronic device with low impedance.

2.3. Capacitive load characteristics of TENG

A single-electrode contact-mode TENG is employed to charge a load capacitor (C_L) to exhibit the capacitive load characteristics in previous work with its equivalent circuit model shown in Fig. 2(b) [47,97]. When the motion of the dielectric reaches its maximum separation distance (i.e. x_{max}), the final voltage and charge on the capacitor can be given by:

$$V(x = x_{max}) = \frac{Q_{SC,max}}{C_L + C_T} \quad (3)$$

$$Q^C(x = x_{max}) = \frac{C_L Q_{SC,max}}{C_L + C_T} \quad (4)$$

While the total stored energy in the capacitor (E_C) can be determined by:

$$E^C = \frac{C_L Q_{SC,max}^2}{2(C_L + C_T)^2} \quad (5)$$

Where Q is defined as the transferred charges, Q_C is the charges stored in the load capacitor, $V_{OC,max}$ and $Q_{SC,max}$ are the open circuit voltage and short circuit transferred charge of the TENG when $x = x_{max}$, respectively.

When C_L is much smaller than the impedance of C_T , the applied voltage on C_L is approximately equal to V_{OC} , while the stored charge is still very small. Instead, when C_L is much larger than the impedance of C_T , the voltage applied on C_L is almost equal to 0. However, the total stored energy is still very small because of the low voltage on C_L . When $C_L = C_{TENG}$, the impedance match state is reached and the maximum value of total stored energy on C_L is obtained.

Similar with the resistive load characteristics, the maximum power when charging a capacitor only reached when the load capacitance is equal to the intrinsic capacitance of TENG. Considering the capacitance of energy storage unit (i.e. much larger than microfarad level) is much larger than the intrinsic capacitance of TENG (usually in nano farad level) [45], the charging efficiency for energy storage unit would be very low.

2.4. V-Q plot of TENG

For quantitatively evaluating and comparing electric performance of TENG, Zi et al. proposed operation cycle using the V-Q plot [50].

The average output power \bar{P} can be used to define the merits of the TENG. Under a certain period of time T , the generated energy per cycle E can be determined as:

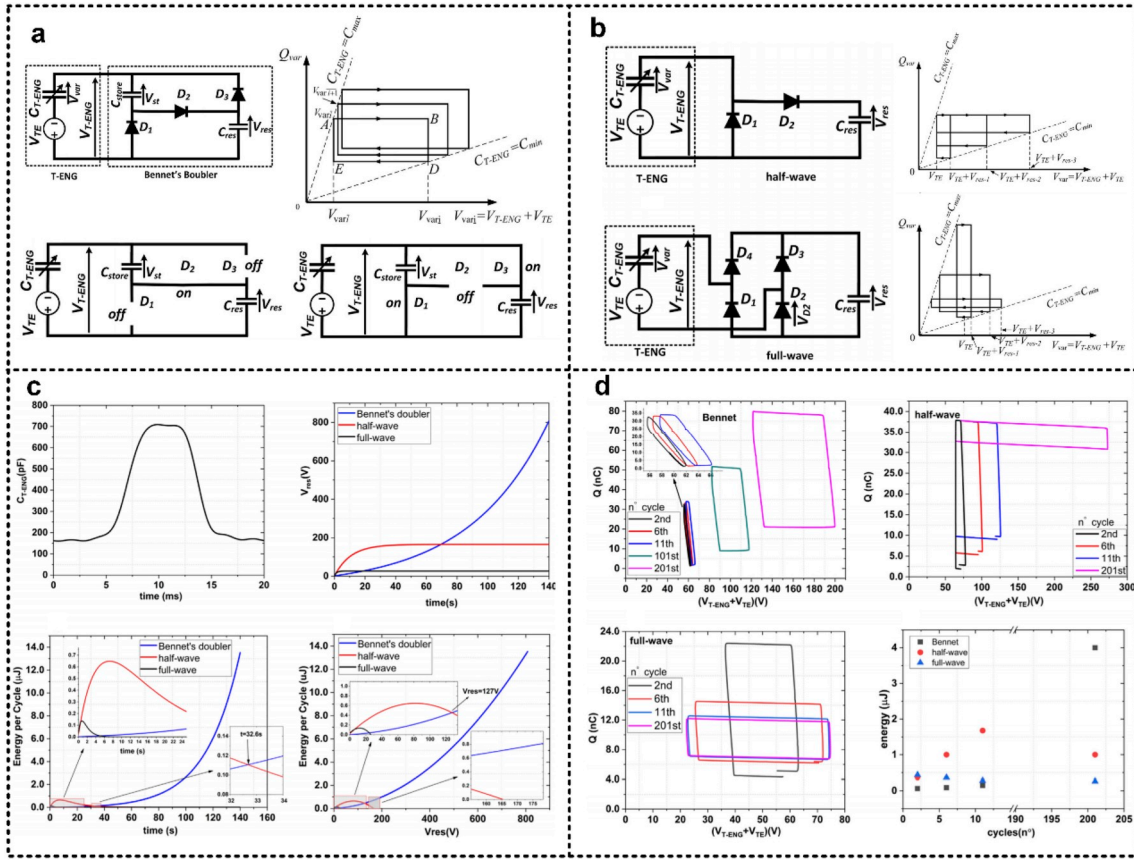


Fig. 6. Bennet's doubler conditioning circuit for TENG. (a) Typical connection of the TENG with the Bennet's doubler circuit to store the output energy in C_{res} , V-Q diagram and corresponding state of the diodes of TENG with Bennet's doubler circuit. (b) Basic diode bridges as conditioning circuits for TENG for the purpose of storing the converted energy in reservoir capacitance of C_{res} and corresponding charge-voltage diagrams. (c) Experimental comparison of the output characteristics of the half and full-wave rectifiers with Bennet's doubler for the $10 \times 10 \text{ cm}^2$ device with contact force of 1.33 N. (d) Comparison of simulated V-Q cycle of the $10 \times 10 \text{ cm}^2$ TENG with the three conditioning circuits. Reproduced with permission [56]. 2018, Elsevier.

$$E = PT = \oint VdQ \tag{6}$$

As an example, a lateral-sliding mode TENG shown in Fig. 2(c) < i > to demonstrate the utilizing of the method. The operation cycle with external load resistance of $100 \text{ M}\Omega$ reaches its steady state after only a few cycles as plotted in Fig. 2(c) < ii > . Meanwhile, the output energy per cycle E can be calculated as the encircled area of the closed loop in the V-Q curve. The steady-state V-Q plots for this LS-mode TENG were also simulated by FEM under various external loads to demonstrate the utilization of the method, as shown in Fig. 2(c) < iii > .

From the encircled areas of these V-Q curves, the output energy per cycle E can be intuitively obtained and compared.

3. Charge boosting for TENG

According to operation cycle of TENG, extracting more charges means obtaining more energy from a TENG. This section would review the recent progresses on charge booting methods for TENG. We would firstly introduce the methods to achieve the cycles for maximized energy output of TENG. Afterwards, the methods for effective energy storage from TENG will be reviewed. For extracting more charges beyond the limit of basic structures of TENG, we will discuss two important achievements using charge pump and Bennet's doubler conditioning circuit.

3.1. Cycles for maximized energy output of TENG

For a specific TENG, the maximized energy in single working cycle can be determined by the cycles for maximized energy output of TENG (CMEO) [50]. A parallel switch with external load is first type circuit that is employed to obtain instantaneous short-circuit conditions as shown in Fig. 3(a). The switch is opened at minimum and maximum displace to enable $Q = Q_{SC,max}$, resulting in the CMEO at infinite load resistances (Fig. 3(b)), which can harvest at least 4 times higher energy than traditional methods. To obtain CMEO at smaller resistance, a serial switch with external load can be used as plotted in Fig. 3(c) [52], which achieved CMEO during 1Ω to $1 \text{ M}\Omega$.

Gang et al. proposed a pulsed TENG with serial mechanical switch to realize CMEO in practical as shown in Fig. 3(d), [51]. In this method, the stored energy in the intrinsic capacitor of TENG would be discharged upon the connection of the switch, the output current is similar with a discharging curve. Different from the standard TENG, the instantaneous output voltage keeps constant in the resistance range from 500Ω to $1 \text{ G}\Omega$ (Fig. 3(e)). Meanwhile, the output current increased as the decreasing of the resistance, leading to much larger instantaneous output power at smaller resistance compared with traditional methods. For a vertical contact-separation mode TENG, the instantaneous output current and power peak can reach nearly 105 and 1010 times of standard TENG at 500Ω , respectively.

A proper triggered switch is the key component for CMEO, but the mechanical switch increases the complexity and fabrication cost of the

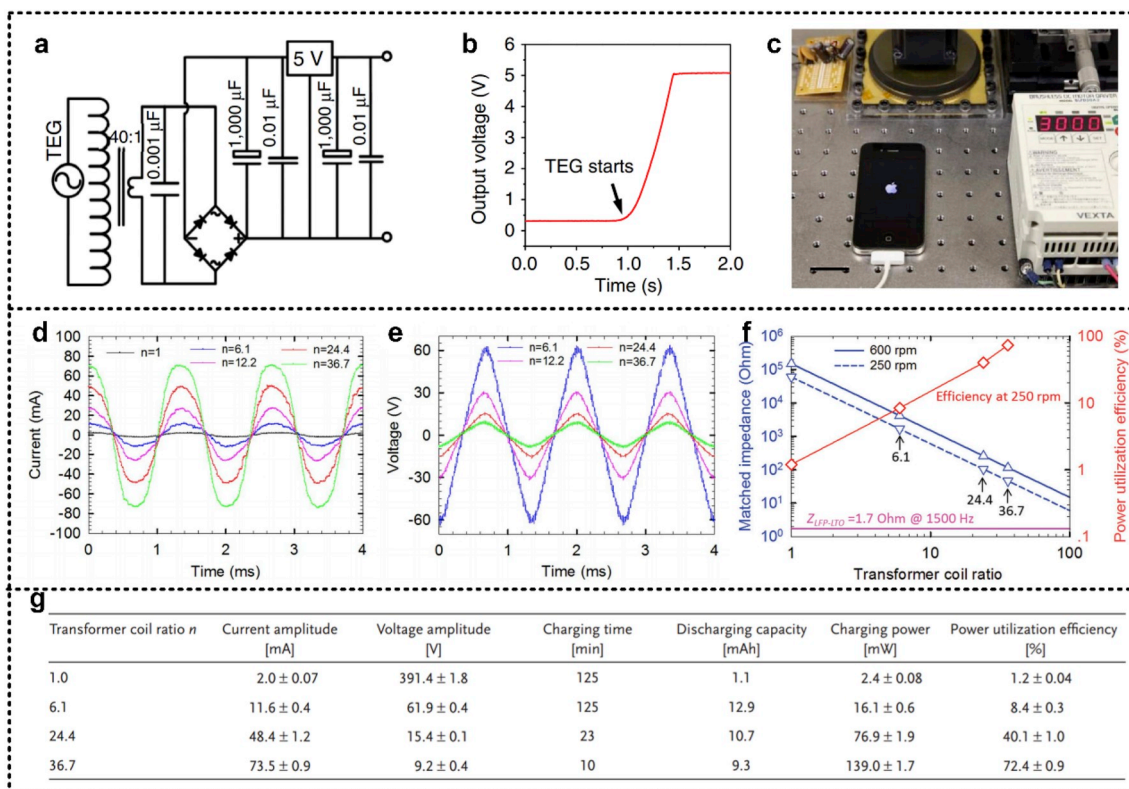


Fig. 7. Inductive transformer for TENG. (a) Circuit diagram of the complete power-supplying system that consists of a triboelectric generator and a power management circuit. (b) Output voltage of the system reaches a constant value of 5 V in less than 0.5 s as the triboelectric generator starts to rotate at 3000 r min⁻¹. (c) Photograph of a cellphone that is being charged by the power-supplying system (scale bar, 3 cm). Reproduced with permission [58]. 2014, Nature. (d–e) Short-circuit current and open-circuit voltage of the TENG at 250 rpm with different transformer coil ratio n . (f) The effect of the transformer coil ratio on matched impedances of the TENG, and the power utilization efficiency of the TENG at 250 rpm when charging a lithium battery. (g) Charging a lithium battery by the TENG with different transformers. Reproduced with permission [59]. 2016, Wiley.

TENG. Self-powered switch triggered by TENG's voltage is a possible solution. For example, an electrostatic vibrator switch and an air-discharge switch with a tip-plate configuration are developed in previous works [98,99], as shown in Fig. 3(f-g), respectively. Driven by the potential difference of TENG itself, these methods could deliver CMEO without increasing the complexity of TENG. However, as driven by the voltage difference, these switches usually are triggered at a specific threshold voltage, which is determined by the parameter of the switch. Therefore, these switches have to be redesigned for a specific TENG for a perfect CMEO.

3.2. Effective energy storage from TENG

The generated energy of TENG is usually rectified by a full-wave rectifier and then stored in a capacitor or battery. V-Q plot can be used to analyze and optimize the charge cycles as shown in Fig. 4(a) [55]. Notably, the transferred charge can't reach 0 and $Q_{SC,max}$ state due to the voltage drop of rectifier and the accumulated voltage on the capacitor, which limited its charging efficiency. By employing a parallel switch with the capacitor, the transferred charge could reach 0 and $Q_{SC,max}$ state, resulting improved energy-storage efficiency (up to 50%, Fig. 4(b)). Fig. 4(c) shows the changes of the charging voltage V_C , the charge flowing to the capacitor per cycle Q_C and the stored energy per cycle versus the number of the charging cycles E_C , respectively. Compared with the direct charging cycle, V_C increases faster, Q_C decreases slower and hence E_C is significantly promoted in the designed charging cycle. The reason of slower decay of Q_C in the designed charging cycle

is during the switch-on operations, the charges are fully transferred to $Q_{SC,max}$ or 0, so that there are more charges available to flow into the capacitor in the next half-cycle.

3.3. Charge pump

Charge density is one of the most important parameters of TENG, since it directly determines the transferred charge and open circuit voltage thus influences output energy in single cycle (i.e. encircle area of V-Q plot). However, the charge density of traditional TENG is restricted by air breakdown, thus the maximum charge density of TENGs working in air environment has been limited to about 250 μCm^{-2} .

Charge pump is a good method to solve this problem [53,54]. The basic structure for charge pump is shown in Fig. 5(a) [54]. As capacitors can take huge quantity of charges under external voltage, and the plane-parallel capacitor has a similar structure with the friction layers, a charge pump is thus composed using a traditional TENG and an inner plane-parallel capacitor structure (PPCS). Traditional TENG is used for generating high voltage under vibration, and filling charge into the PPCS through a full-wave rectifier. Then the outer electrodes of PPCS are connected with external circuit via another full-wave rectifier for exporting electrical energy when the device is driven by vibration.

Through this design, the output current and effective charge density are increased to 10.32 and 7.22 times that of part I, and a maximum effective charge density of 490 μCm^{-2} is obtained.

Adopting similar structure, Liang et al. reached a highest charge density of 1020 μCm^{-2} in their work as shown in Fig. 5(b) [53]. This

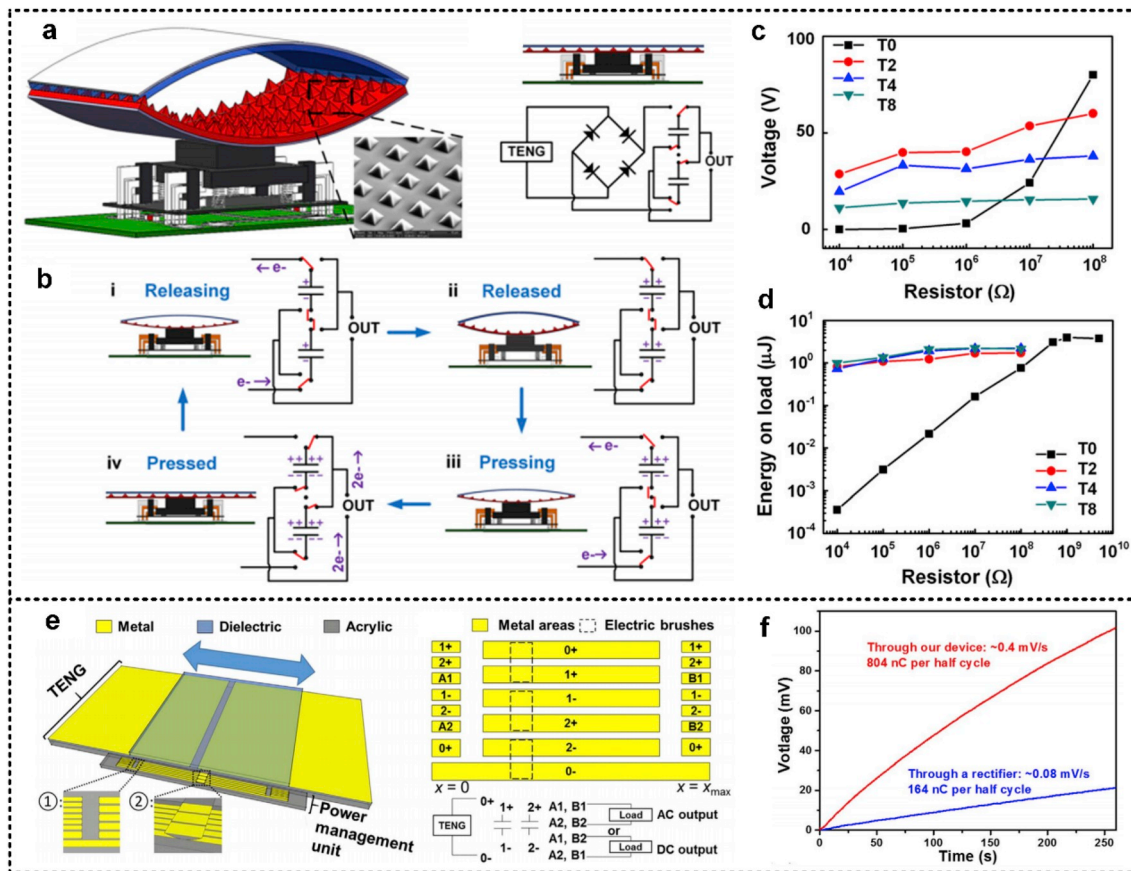


Fig. 8. Capacitive transformer for TENG. (a) 3D structure of the PTM-TENG, and the pressed PTM-TENG's cross sectional view and the equivalent circuit diagram. (b) A full working cycle of the PTM-TENG. (c) Output voltages of the T0, T2, T4, and T8 under various load resistances. (d) Output energy (energy supplied to the load) of the T0, T2, T4, and T8 under various load resistances. Reproduced with permission [61]. 2014, IOPscience. (e) The auto-power-management design and the motion-triggered unit. (f) The charging plots of a 5 mF supercapacitor. Reproduced with permission [60]. 2017, Elsevier.

enhancement may be attributed to the single layer dielectric material in the inner capacitor and the fuller contact of flat structure.

3.4. Bennet's doubler conditioning circuit

Bennet's doubler conditioning circuit, working on the principles of Bennet's doubler device, is proved to be another effective circuit for TENG [56,57,100], with the advantage of simple diagram and less components. No mechanical switch or external control is required to store the harvested energy in a reservoir capacitor. Typical connection of TENG with the Bennet's doubler circuit to store the output energy in C_{res} , and V-Q plot and corresponding state of the diodes of TENG with Bennet's doubler circuit are shown in Fig. 6(a). Using this circuit, the encircled area of V-Q plot would increase exponentially with working cycles, resulting in exponentially increased energy to be store in C_{res} , as long as the ratio of the largest capacitance and smallest capacitance of TENG is larger than 2 [56].

As comparisons, the circuit diagrams and V-Q plots when charging using half-wave and full-wave rectifier are shown in Fig. 6(b), respectively. When charging for same capacitor C_{res} , half-wave rectifiers and full-wave rectifiers quickly charge the reservoir capacitance C_{res} to a moderate saturation value, 165 V and 26 V, respectively, but the Bennet's doubler performance rises up to 835 V after 140 s as plotted in Fig. 6(c). Fig. 6(d) compares the delivered energy at various cycles between the three circuits by V-Q plots, showing again that the diode bridge behaves better than the Bennet doubler only at the beginning of

the conversion process.

4. Buck converting for TENG

TENG usually has a high voltage of typically hundreds of volts and low output current. Therefore, buck converting for TENG is one of most important processes for managing electric output of TENG. We will review the recently achievements in buck converting for TENG in this section, which includes inductive transformer, capacitive transformer, universal strategy with active switch and universal strategy with passive switch.

4.1. Inductive transformer

Inductive transformer is a common method for dropping voltage, which is also employed to reduce the high voltage from TENG by previous works [58,59,101–105]. Zhu et al. presented a power management circuit consisting of a transformer, a rectifier, a voltage regulator and capacitors, which was diagrammed in Fig. 7(a) [58]. Using this circuit, the high voltage from TENG can be reduced. Then the circuit can produce a direct current (DC) output at a voltage of 5 V in 0.5 s after the TENG begins to work (Fig. 7(b)). Since 5 V serves as a standard charging voltage for many commercial portable electronics, a cellphone automatically opened once the voltage output reaches 5 V due to the working of the TENG, as diagrammed in Fig. 7(c).

The coil turn ratio of the transformer is the key factor deciding its

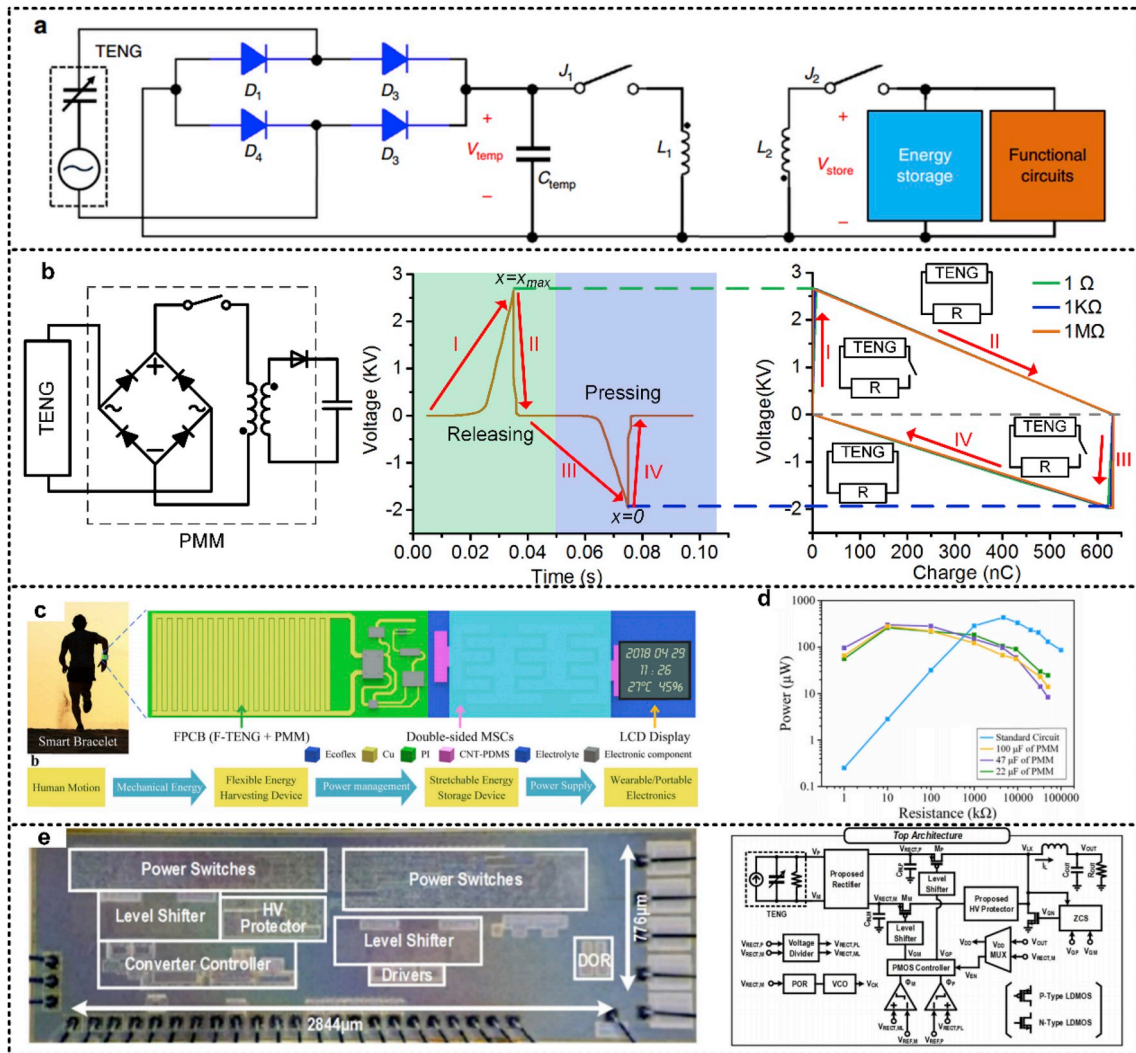


Fig. 9. Universal strategy with active switch for TENG. (a) Circuit diagram of the power management circuit. Reproduced with permission [62]. 2015, Nature. (b) A two steps strategies and PMM for TENG. Reproduced with permission [52]. 2017, Elsevier. (c) Schematic diagram of high-efficiency self-charging smart bracelet configured with power management module on flexible substrate. (d) The AC power curve of F-TENG and experimental DC power curve via PMM for different capacitors. Reproduced with permission [107]. 2019, Elsevier. (e) Die micrograph and top architecture of the integrated energy harvesting circuit for TENG. Reproduced with permission [108]. 2018, IEEE.

performance. Previous work utilized transformers with different coil ratios to tune the voltage, current and charging efficiency of TENG, as shown in Fig. 7(d-g) [59]. When the coil ratio was increased from $n = 1$ to 36.7, the current amplitude rose from 2.0 mA to 73.5 mA, respectively. Corresponding voltage amplitude was then decreased from 391.4 V to 9 V, respectively. Meanwhile, the charging efficiency by a transformer with coil ratio of 36.7 can be significantly improved from 1.2% to about 72.4%.

A transformer was also found to be effective to decrease the large impedance of TENG. By a transformer with coil ratio of n , the impedance will be decreased to $Z_1 = n^{-2}Z_0$. In their work, with a transformer ($n = 36.7$), the matched impedance decreased to about 110 Ω, as plotted in Fig. 7(f), [59].

When employed as the PMM for TENG, Inductive transformer shows the advantage of reducing the voltage as well as the matched impedance, resulting in higher current and power utilization efficiency. However, as the transformer has a center frequency, the transformer efficiency would dramatically decrease when off the center frequency. The transformer only suits for the rotary-mode TENG with a relatively high and stable working frequency.

4.2. Capacitive transformer

Different from the inductive transformer working at a typical frequency, a capacitive transformer with an array of self-connection switch can be utilized for managing the short pulse at variable frequency output of a TENG [60,61]. By integrating a contact-separation-mode TENG with an array of self-connection-switching capacitors that are connected in serial when being charged and then in parallel during discharging, they developed a power-transformed-and-managed TENG (PTM-TENG) as shown in Fig. 8(a-b). It was found that the PTM-TENG's output voltage can be tunably decreased, while its output current and charges can be increased at the same time. When there are N capacitors in the circuit, the output charges and voltage can be determined as follows:

$$Q_{out} = NQ_0$$

$$V_{out} = \frac{V_0}{N} \tag{7}$$

Where V_0 and Q_0 represent the total generated charges voltage and charges in the serial capacitors. Their experimental results validated

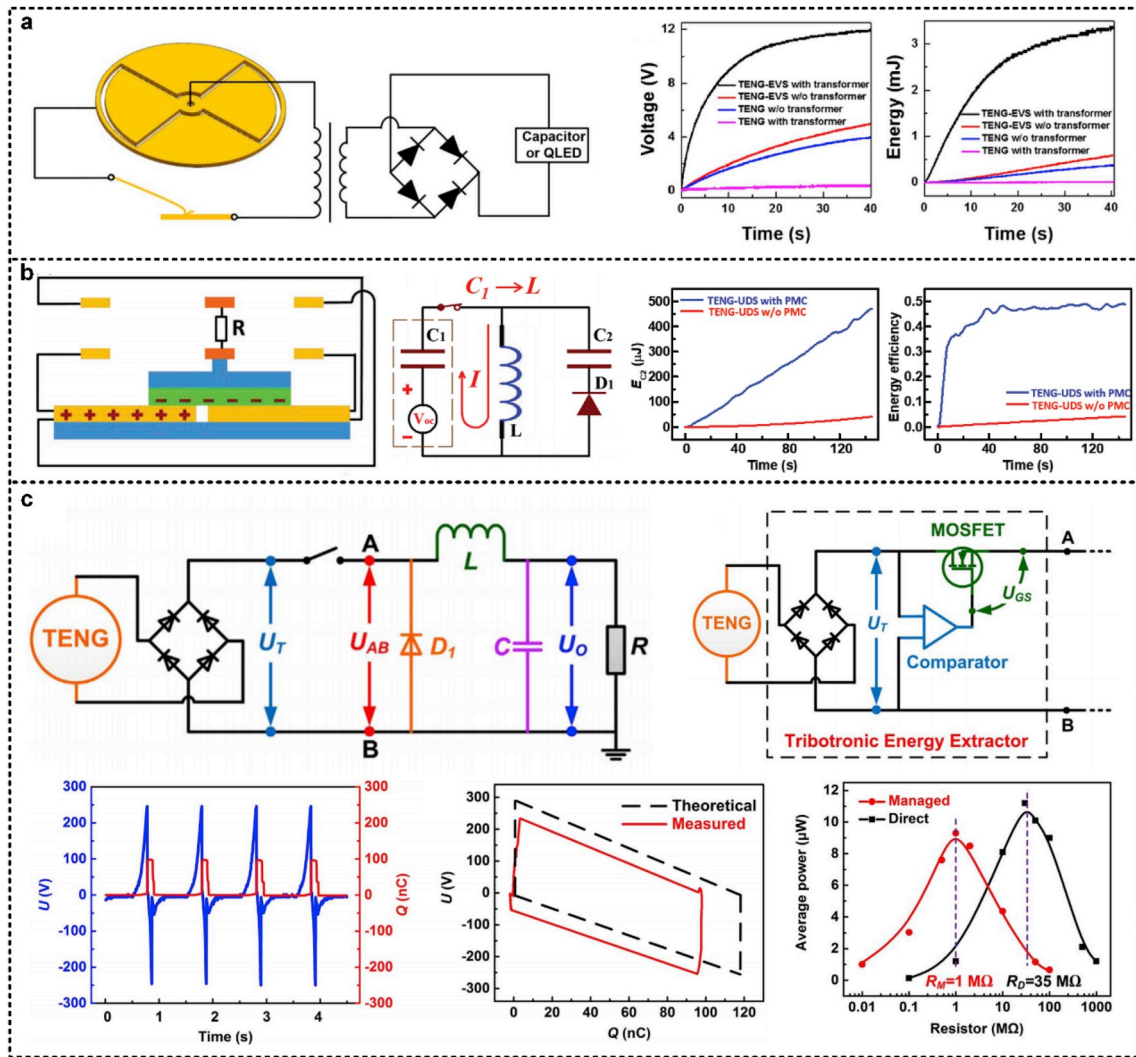


Fig. 10. Universal strategy with passive switch for TENG. (a) Using an electrostatic vibrator switch. Reproduced with permission [109]. 2018, Elsevier. (b) Using a unidirectional mechanical switch. Reproduced with permission [63]. 2018, ACS. (c) Using the tribotronic energy extractor and a MOSFET switch, which includes a rectifier, a voltage comparator and a MOSFET switch. The energy is autonomously transferred by self-management mechanism without external power supply. Reproduced with permission [64]. 2018, Elsevier.

above equations as shown in Fig. 8(c-d), which realize the purpose of reducing the voltage. Zi et al. designed similar solutions for sliding-mode TENG as shown in Fig. 8(e-f), which shown much high charging speed for a 5 mF supercapacitor and obtained a maximum efficiency of 25% [60].

However, Because of the complex mechanical layout, this design has limited the number of switch and transformer ratio.

4.3. Universal strategy with active switch

For improving the universality of the power management circuit for TENG, Niu et al. designed the following charging strategy for maximized energy storage efficiency [62].

This theoretical charging cycle was realized by a two-stage power management circuit in their work, as shown in Fig. 9(a). At the first stage, a temporary capacitor C_{temp} is charged by a TENG through a bridge rectifier. The second stage is to transfer the energy from C_{temp} to the final energy storage unit. Since transferring electrostatic energy directly from a small capacitor to a large capacitor (or a battery) results in huge energy loss, two automatic electronic switches and a coupled inductor are utilized in the second stage [106]. Using this circuit, they

successfully converted the pulsed output from a TENG to DC output with the total power efficiency of 59.8%.

Simpler method is proposed in previous work without using the temporary capacitor [52]. A two steps strategy is proposed and adopted: (1) Maximizing the output energy of a TENG by using built-up voltage V_{total} transferred charges Q plot applicable to both-modes TENG; (2) Maximizing the transferred energy from TENG to energy storage unit by employing the LC oscillating model (Fig. 9(b)). It's worth mentioned that both the uniform output from lateral-sliding mode TENG and the pulsed output from contact-separation mode TENG are successfully managed and converted to DC output, demonstrating its universality. Using this method, the total efficiency of PMM was calculated to be 75.5%.

To integrate with TENG, researchers have tried to fabricate PMM on flexible substrate using flexible printed circuit board (FPCB) process as well as silicon wafer using CMOS process for better integration with TENG as shown in Fig. 9(c-e) [107,108].

4.4. Universal strategy with passive switch

Though the total efficiency is relatively high and achieved a practical level, the switch is usually controlled by logic circuit in these

Table 1
Summary and comparison of existing methods for power management of TENG [51–56,58–64,98,99].

Sub-Section	Methods	Improvement/Efficiency (%)	Pros	Cons
Charge boosting	CMEQ	At least 4 times higher energy than traditional methods and much higher improvement at small resistance.	Maximized energy output, Decreased equivalent resistance with serial switch, Suitable for pulsed output of TENG	Needing for a switch triggered by TENG's voltage or motion, Increased equivalent resistance by parallel switch.
	Effective energy storage from TENG	The maximum energy storage efficiency higher up to 50% compared with rectifier.	Improved energy storage efficiency than rectifier, Suitable for pulsed output of TENG	Needing for a switch triggered by TENG's voltage or motion.
Buck converting	Charge pump	Nearly ten times improvement of surface charge density.	Ultrahigh surface charge density, Without switch, Suitable for pulsed output of TENG	More complicated structure than traditional TENG, Needing for additional rectifier.
	Banner's doubler circuit	Exponentially amplifies the output electrical energy.	Without switch, Exponentially amplifies output. Suitable for pulsed output of TENG	Relatively low output at initial cycles.
Universal strategy with active switch	Inductive transformer	1.2%–72.4%	Without switch, Simple structure.	Not suitable for pulsed output of TENG.
	Capacitive transformer	25%	Suitable for pulsed output of TENG	Increased complexity with voltage drop ratio.
	Universal strategy with active switch	59.8%–75.5%	Suitable for pulsed output as well as uniform output of TENG, High efficiency	Active switch controlled by logic circuit.
	Universal strategy with passive switch	48%–85%	Suitable for pulsed output as well as uniform output of TENG, High efficiency, Not needing for logic circuit.	Passive switch triggered by TENG's motion or voltage, which needs customization for a specific TENG.

works. Typically, the logic circuit is powered by outer power [52,106], which limited its application when starting the energy harvesting system without battery or any initial energy. In this regard, mechanical switch or self-powered switch would be a good candidate.

As an example, an electrostatic vibrator switch was introduced as a self-powered switch of a TENG as shown in Fig. 10(a) [109], where its vibrating is driven by the potential difference of the TENG itself. Using this switch, the output voltage and output energy of the TENG can be maximized. Also, a circuit with enhanced powering ability for a capacitor based on the self-powered switch is developed in their work. Mechanical switch triggered by TENG's motion is also developed using a unidirectional switch and an inductor as shown in Fig. 10(b) [63], which reached an energy storage efficiency of 48.0% in the actual experiments.

Xi et al. reported a passive autonomous switch made up of a low-power voltage comparator and a MOSFET switch as shown in Fig. 10(c) [64]. A reference voltage for comparator is set according to maximum output voltage of TENG. When the voltage of TENG is larger than this reference voltage, the comparator would deliver a high voltage to open the MOSFET switch. Therefore, the switch could automatically turn on when the voltage of TENG reaches its peak value. Accordingly, they proposed a tribotronic energy extractor based on the autonomous switch and rectifier to maximally obtain energy from TENG and transfer to the back-end circuit autonomously. Using this circuit, a maximum energy extract efficiency of 84.6% could be achieved from the comparison of the measured and theoretical V-Q plot. With the implemented power management module, about 85% energy can be autonomously released from the TENG and output as a steady and continuous DC voltage on the load resistance, which is the highest efficiency to the best of my knowledge.

Table 1 summarizes a comparisons of published reports for power management of TENG including charge boosting and buck converting methods [51–56,58–64,98,99]. For a given TENG, CMEQ can extract maximum energy in single cycle, while Bennet's doubler conditioning circuit could significantly improve the stored energy by exponentially output for long term charging. Charge pump is a novel and powerful tool to increase the output power of TENG itself. For buck converting methods, inductive transformer is still an ideal tool for TENG with uniform and fixed center frequency such as rotary mode TENG. When TENG generated pulsed output with random frequency, universal strategies with active/passive switch have much better performance.

5. Energy storage for TENG and applications

Energy generation and storage are the two most important areas for developing new power sources, while power management module serves as a bridge for these two components [10,13,110,111]. For powering portable and wearable electronics, rechargeable batteries or capacitors are still indispensable considering the discontinuity output of TENG. This section would review the recent progress on the energy storage of TENG including charging battery and supercapacitor (SC). Potential applications enabled by the utilization of power management and energy storage also will be covered.

5.1. Battery

The first power storage unit employed for storage the charged electric energy of TENG is battery [78,80,82–84,112,113], which is the most used power storage unit in the traditional electronics as we all know. Wang et al. demonstrated the first flexible self-charging power unit (SCPU) in 2013 by integrating a TENG-based mechanical energy harvester and a Li-ion battery (LIB) based energy storage, which is capable of simultaneously harvesting and storing ambient mechanical energy [80] (Fig. 11(a)). In their work, the LIB can be directly charged by electricity produced by TENG under the mechanical motions. When the surrounding mechanical energy is applied onto the SCPU, an

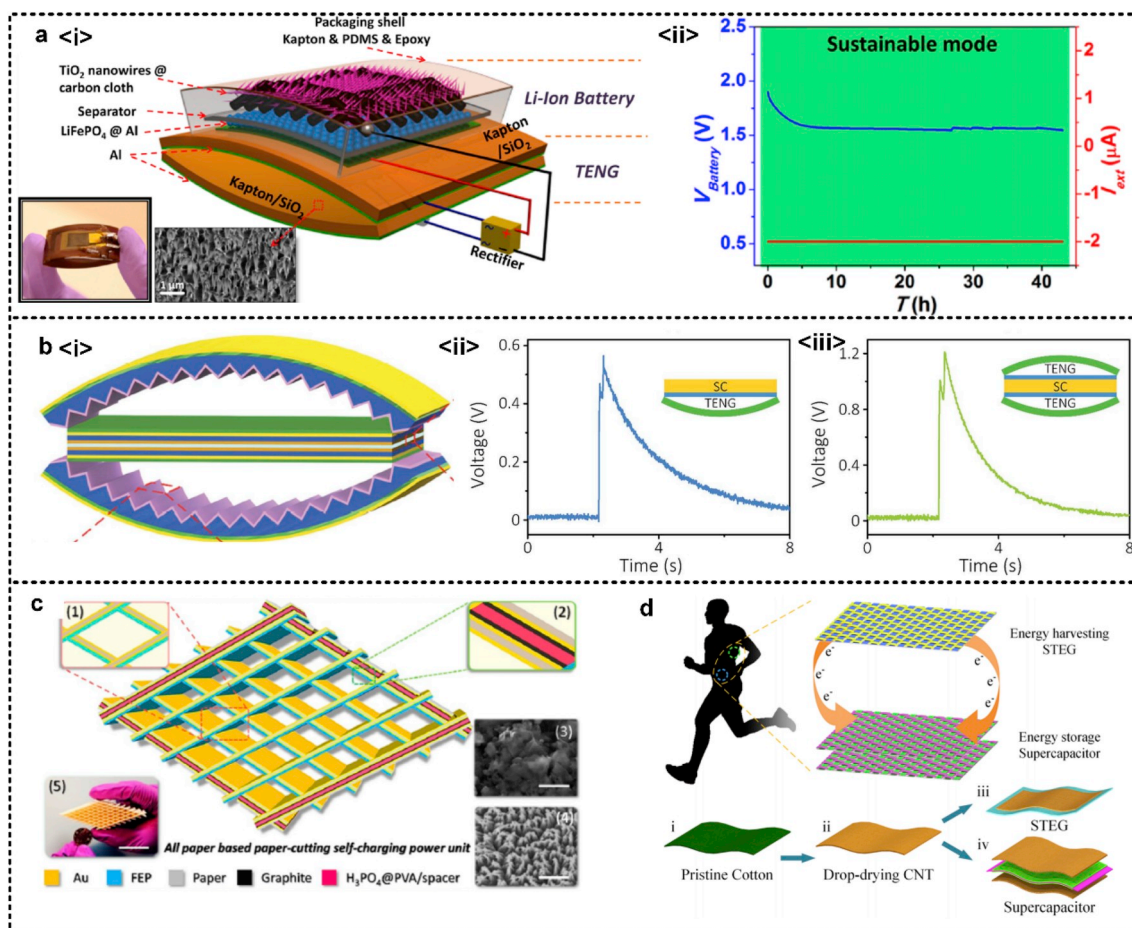


Fig. 11. Energy storage for TENG. (a) Structure design of a flexible self-charging power unit. Reproduced with permission [80]. 2013, ACS. (b) The structure design of sandwich-shaped SCPU, and the charging curve of a 1 μF capacitor of a single TENG and 2-parallel connection TENGs, respectively. Reproduced with permission [91]. 2016, The Royal Society of Chemistry. (c) Schematic illustration of the all-paper-based cut-paper self-charging power unit. Reproduced with permission [88]. 2017, ACS. (d) Schematic of the all-fabric-based self-charging power cloth, which is made of a wearable STEG and a flexible supercapacitor. Adapted from Ref. [79] with permission. Reproduced with permission [79]. 2017, AIP Publishing.

alternating current is generated. After rectification, the electrical energy can be stored in the LIB, which can be fully charged in 11 h. Additionally, a new “sustainable mode” is proposed for a power source in their work, in which the environment mechanical energy is scavenged to charge the battery while the battery keeps driving an external load as a DC source. In this mode, the demonstrated SCPU can provide a continuous and sustainable DC current of 2 μA at a stable voltage of 1.55 V for as long as there is mechanical motion/agitation. Notably, the LIB in the SCPU serves not only as energy storage, but also as a power regulator and management for the entire system by utilizing the stable electrode-potential difference of LIB [113].

5.2. Supercapacitor

How to integrate the two device well is the first issue to be solved for using SC to store the energy of TENG. Song et al. proposed a hybrid sandwich-shaped self-charging power unit [91]. They integrated two arch-shaped TENG and carbon nano tube (CNT) based solid-state SC. Through a novel TENG-SC-TENG design, their device could take advantages of both the top and bottom surfaces of SC and greatly decrease the unit's volume as shown in Fig. 11(b). When compressive stress is applied to the SCPU, the mechanical energy is directly converted into electrical energy and stored in the SC efficiently. The integrated sandwich-shaped SCPU in their work obtained enhanced performance. It could charge the same 1 μF capacitor to 1.2 V through a full-wave

rectifier in a single cycle, obtaining more than doubles transferred charges compared with the single arch-shaped TENG.

When TENG integrating with SC, the total weight and volume are very important, which require the substrate to be flexible and lightweight. An ultralight cut-paper based self-charging power unit that is capable of simultaneously harvesting and storing energy by combining a cut-paper-based TENG and a paper-based supercapacitor (Fig. 11(c)), [88]. Utilizing paper as the substrate for both the TENG and SC makes the complete power unit lightweight and flexible. The assembled cut-paper structure was designed to integrate plenty of rhombic-shaped TENG units in a certain volume so as to lower the output voltage and raise the output charge quantity. With a suitable capacitance of ~ 1 mF, the SC is effectively charged to ~ 1 V within 250 s by TENG in their work.

For wearable electronics, the fabric is an ideal material for energy devices since people wear clothes every day. Song et al. presented a prototype of all-fabric-based self-charging power cloth by integrating a wearable single-electrode triboelectric generator (STEG) and a flexible supercapacitor with a general CNT/cotton fabric electrode (Fig. 11(d)), [79]. Multiwalled CNT is selected to compound with the cotton fabric and served as the electrode of STEG. By attaching among the cloth the body motion energy could be scavenged by the STEG and stored in the supercapacitors. This work demonstrates novel method of realizing high integration and working compatibility for supplying power for wearable electronics.

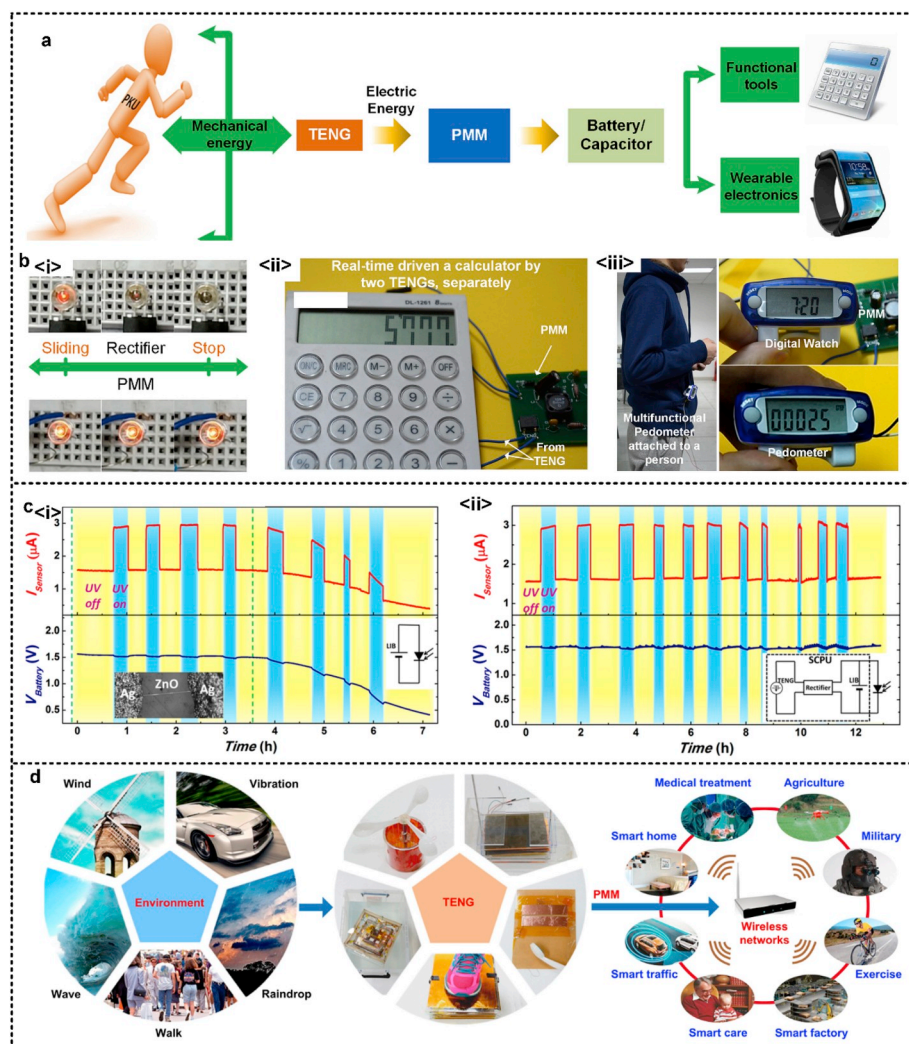


Fig. 12. Applications of TENG using PMM and energy storage unit. (a) TENG based energy flow chart for scavenging mechanical energy to power electronics. (b) Comparison of using TENG to power a red LED via a commercial rectifier and PMM, and real-time driven commercial electronics by two modes TENGs via PMM, separately. (d) Supplying power for a multifunctional pedometer. Reproduced with permission [52]. 2017, Elsevier. (c) Operation of the UV sensor when solely driven by the LIB part in the SCPU, and the operation of the UV sensor continuously driven by the SCPU in the “sustainable mode” for ~13 h. Reproduced with permission [80]. 2013, ACS. (d) Environmental mechanical energy harvesting by various TENGs with the PMM, such as human walking, natural wind, vibration, wave and raindrop for distributed wireless sensor networks and future Energy Internet. Reproduced with permission [64]. 2018, Elsevier.

5.3. Applications

The power management method for TENG has achieved dramatically improvement, and the highest power conversion efficiency of PMM till now is 85%, which could significantly broaden the application areas of TENG. An example of energy flow chart for scavenging mechanical energy to power electronics is diagramed in Fig. 12(a) [52]. By combing the PMM with TENG, the pulsed output of TENG can be efficiently converted to DC output and power electronic device in real-time, forming a totally self-powered system. As an example, when directly powering a red LED bulb via a rectifier using TENG, the LED bulb would be illuminated instantaneously as shown in Fig. 12(b). But using the PMM to power this LED, it would be continuously turned on with enhanced brightness. Meanwhile, a commercial calculator and a multifunction pedometer were successfully driven at a very low working frequency of TENGs (< 2 Hz) for demonstrating the continuously supplying power for commercial electronics using TENG.

PMM has significantly improved the energy conversion efficiency between TENG and energy storage unit, which exhibited the ability to continuously supply power for commercial electronics. But when the mechanical energy doesn't exist or the average power isn't sufficient for the working of commercial electronics, the power supply would become invalid. On the other hand, relatively large energy storage unit, such as battery and supercapacitor, can store the electric energy from TENG and supply power for electronics when needed, which could greatly expand its application scenarios.

Sihong et al. demonstrated SCPU under the “sustainable mode” can serve as a nonstop power source as shown in Fig. 12(c), [80]. After the battery of the SCPU fully charged, it was used to power the ultraviolet (UV) sensor. This battery could remain a stable voltage of 1.53 V for the periodically working of UV light without charging by TENG. When the LIB was being charged by the TENG under a frequency of 9 Hz while driving the UV sensor, the output voltage of the battery can stay at the plateau of around 1.55 V for over 12 h, during which the UV light was periodically turned on and off for more than 10 times without obvious decay in current level.

With the PMM and energy storage, various kinds of mechanical energy can be efficiently scavenged by TENGs, such as human walking, natural wind, vibration, wave and raindrop. Fengben et al. gives a summary of using TENGs with PMM to harvesting the mechanical energy existed in the environment [64]. By harvesting human kinetic and environmental mechanical energy, and converting the pulsed output from TENG to DC power using PMM, then storing the electric energy in battery/SC, the PMM and energy storage unit for TENG are promising for a complete sustainable energy solution for wearable electronics, distributed wireless sensor networks and future Energy Internet.

6. Summary and prospective

Power management for TENG is one of the most urgent issues to be resolved for its practical applications, which has obtained significantly improvement through the last few years' productive world-wide

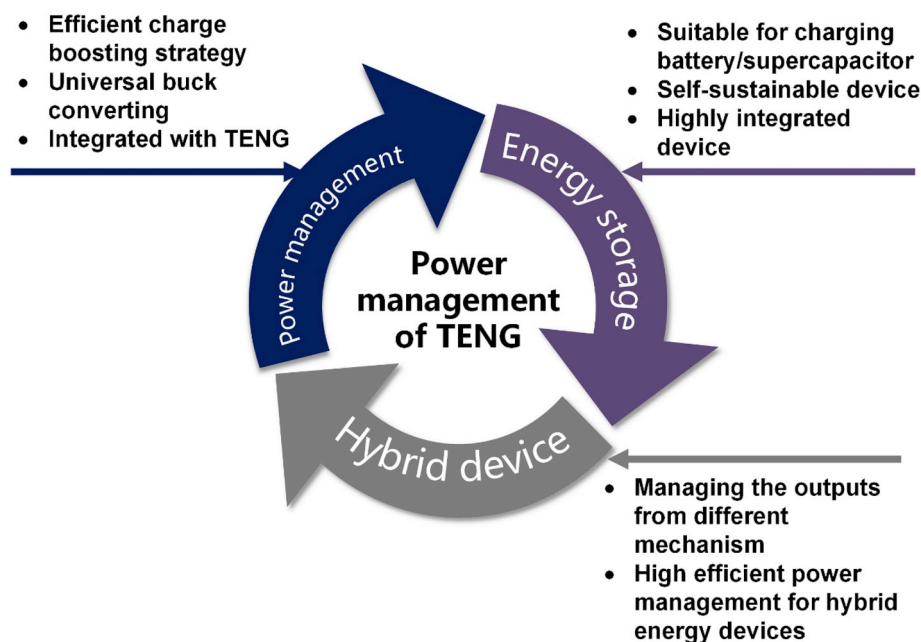


Fig. 13. Prospective for power management of TENG.

research works. Theoretical model, and different load characteristics have been reviewed, and V-Q plot is proved to be a useful tool for analyses the performance of TENG. For management the output of TENG, charge boosting, buck converting and energy storage are three processes need to be considered, while all of which have achieved significant improvement in the past few years. However, TENG and its power management system are still not available for practical applications. As toward future applications using TENG as a sustainable power source, there are a number of issues and problems need to be addressed as diagramed in Fig. 13.

First, the power management of TENG needs to be further optimized. Charge boosting decides the maximum energy we can extract from TENG, which need to be further enhanced for efficient charge boosting strategies suitable for all-modes TENG. Though the universal strategy exhibited high efficiency as well as universality to different modes TENG. The controlling circuit in most of these solutions were powered by outer circuit, and the efficiency of self-powered switch is relative low. Therefore, a high efficiency and passive PMM is still of great urgency for TENG, which we believe may be solved by exploiting the basic model of TENG. For wearable applications, the size of PMM still need to be reduced, and its substrate need to be replaced by flexible material to integrate with TENG.

Secondly, PMM needs to be optimized for supercapacitor/battery. Though existing PMMs show high efficiency for commercial capacitor, an efficient PMM for SC/battery is still need to be developed considering the different mechanisms with traditional capacitor. SCPU is proposed for sustainable working of electronics, with the development of PMM, a totally self-sustainable system has great potential to be developed in the future. Besides, the energy storage unit of SCPU need to be designed to better integrated with TENG and PMM needs to be optimized for supercapacitor/battery for a sustainable power source. TENG has the advantages of highly flexibility and stretchability. To integrate energy storage unit and TENG together, energy storage unit should have the same property with TENG. Different from traditional battery with large capacity, the capacity of energy storage unit for TENG should adjust according to the application scenario as well as the output performance of TENG.

Thirdly, PMM suitable for hybrid energy cell needs to be developed. By integrating TENG with other mechanism devices, such as

electromagnetic induction, piezoelectric effect, thermoelectric effect, photovoltaic effect, etc., hybrid energy cells are to develop a technology to individually or simultaneously scavenge multi-mode energies from environment, so that the sensors or other devices can be powered by using whatever energy that is available at their working environment [114–118]. This kinds of harvesters have received a lot of attention and rapid development in the recent years [118–122]. Therefore, proper PMMs are of great urgency to be developed for managing the electric energy from different mechanisms.

Acknowledgements

This work was supported by National Key R&D Project from Minister of Science and Technology, China (2016YFA0202701, 2016YFA0202704) and the National Natural Science Foundation of China (Grant No. 61674004, 61176103 and 91323304).

References

- [1] J.A. Rogers, T. Someya, Y. Huang, *Science* 327 (2010) 1603–1607.
- [2] H. Chen, Z. Su, Y. Song, X. Cheng, X. Chen, B. Meng, Z. Song, D. Chen, H. Zhang, *Adv. Funct. Mater.* 27 (2017) 1604434.
- [3] J. Gubbi, R. Buyya, S. Marusic, M. Palaniswami, *Future Gener. Comput. Syst.* 29 (2013) 1645–1660.
- [4] S.K. Kang, R.K. Murphy, S.W. Hwang, S.M. Lee, D.V. Harburg, N.A. Krueger, J. Shin, P. Gamble, H. Cheng, S. Yu, Z. Liu, J.G. McCall, M. Stephen, H. Ying, J. Kim, G. Park, R.C. Webb, C.H. Lee, S. Chung, D.S. Wie, A.D. Gujar, B. Vemulapalli, A.H. Kim, K.M. Lee, J. Cheng, Y. Huang, S.H. Lee, P.V. Braun, W.Z. Ray, J.A. Rogers, *Nature* 530 (2016) 71–76.
- [5] S. Xu, Y. Zhang, J. Cho, J. Lee, X. Huang, L. Jia, J.A. Fan, Y. Su, J. Su, H. Zhang, H. Cheng, B. Lu, C. Yu, C. Chuang, T.I. Kim, T. Song, K. Shigeta, S. Kang, C. Dagdeviren, I. Petrov, P.V. Braun, Y. Huang, U. Paik, J.A. Rogers, *Nat. Commun.* 4 (2013) 1543.
- [6] N.S. Choi, Z. Chen, S.A. Freunberger, X. Ji, Y.K. Sun, K. Amine, G. Yushin, L.F. Nazar, J. Cho, P.G. Bruce, *Angew. Chem. Int. Ed. Engl.* 51 (2012) 9994–10024.
- [7] J. Pu, X. Wang, R. Xu, S. Xu, K. Komvopoulos, *Microsystems & Nanoengineering* 4 (2018) 16.
- [8] S.P. Beeby, M.J. Tudor, N.M. White, *Meas. Sci. Technol.* 17 (2006) R175–R195.
- [9] Z.L. Wang, *Adv. Funct. Mater.* 18 (2008) 3553–3567.
- [10] Z.L. Wang, J. Chen, L. Lin, *Energy Environ. Sci.* 8 (2015) 2250–2282.
- [11] Z.L. Wang, *ACS Nano* 7 (2013) 9533–9557.
- [12] F.R. Fan, Z.Q. Tian, Z.L. Wang, *Nanomater. Energy* 1 (2012) 328–334.
- [13] Z.L. Wang, *Faraday Discuss* 176 (2015) 447–458.
- [14] X. Cheng, B. Meng, X. Chen, M. Han, H. Chen, Z. Su, M. Shi, H. Zhang, *Small* 12

- (2016) 229–236.
- [15] X.L. Cheng, Z.J. Song, L.M. Miao, H. Guo, Z.M. Su, Y. Song, H.X. Zhang, *J. Microelectromech. S* 27 (2018) 106–112.
- [16] X.S. Zhang, M.D. Han, B. Meng, H.X. Zhang, *Nanomater. Energy* 11 (2015) 304–322.
- [17] H. Ryu, J.H. Lee, T.Y. Kim, U. Khan, J.H. Lee, S.S. Kwak, H.J. Yoon, S.W. Kim, *Adv. Energy Mater.* 7 (2017) 1700289.
- [18] X.-S. Zhang, M.-D. Han, R.-X. Wang, F.-Y. Zhu, Z.-H. Li, W. Wang, H.-X. Zhang, *Nano Lett.* 13 (2013) 1168–1172.
- [19] W. Tang, B. Meng, H. Zhang, *Nano Energy* 2 (2013) 1164–1171.
- [20] F.R. Fan, L. Lin, G. Zhu, W.Z. Wu, R. Zhang, Z.L. Wang, *Nano Lett.* 12 (2012) 3109–3114.
- [21] M. Shi, H. Wu, J. Zhang, M. Han, B. Meng, H. Zhang, *Nano Energy* 32 (2017) 479–487.
- [22] X. Chen, Y. Song, H. Chen, J. Zhang, H. Zhang, *J. Mater. Chem. A* 5 (2017) 12361–12368.
- [23] X.L. Cheng, Y. Song, M.D. Han, B. Meng, Z.M. Su, L.M. Miao, H.X. Zhang, *Sensor Actuat. a-Phys* 247 (2016) 206–214.
- [24] H. Wu, H. Guo, Z. Su, M. Shi, X. Chen, X. Cheng, M. Han, H. Zhang, *J. Mater. Chem. A* 6 (2018) 20277–20288.
- [25] H. Wu, Z. Su, M. Shi, L. Miao, Y. Song, H. Chen, M. Han, H. Zhang, *Adv. Funct. Mater.* 28 (2018) 1704641.
- [26] J. Zhang, Z. Song, H. Guo, Y. Song, B. Yu, H. Zhang, *IEEE Trans. Nanotechnol.* 17 (2018) 460–466.
- [27] Z. Su, M. Han, X. Cheng, H. Chen, X. Chen, H. Zhang, *Adv. Funct. Mater.* 26 (2016) 5524–5533.
- [28] M. Han, B. Yu, G. Qiu, H. Chen, Z. Su, M. Shi, B. Meng, X. Cheng, H. Zhang, *J. Mater. Chem. A* 3 (2015) 7382–7388.
- [29] X.L. Cheng, L.M. Miao, Z.M. Su, H.T. Chen, Y. Song, X.X. Chen, H.X. Zhang, *Microsystems & Nanoengineering* 3 (2017).
- [30] X.-S. Zhang, M. Su, J. Brugger, B. Kim, *Nano Energy* 33 (2017) 393–401.
- [31] X.-S. Zhang, J. Brugger, B. Kim, *Nano Energy* 20 (2016) 37–47.
- [32] J. Chen, J. Yang, Z.L. Li, X. Fan, Y.L. Qi, Q.S. Jing, H.Y. Guo, Z. Wen, K.C. Pradel, S.M. Niu, Z.L. Wang, *ACS Nano* 9 (2015) 3324–3331.
- [33] Z.L. Wang, T. Jiang, L. Xu, *Nanomater. Energy* 39 (2017) 9–23.
- [34] U. Khan, S.W. Kim, *ACS Nano* 10 (2016) 6429–6432.
- [35] Y. Yang, G. Zhu, H.L. Zhang, J. Chen, X.D. Zhong, Z.H. Lin, Y.J. Su, P. Bai, X.N. Wen, Z.L. Wang, *ACS Nano* 7 (2013) 9461–9468.
- [36] L. Zhang, B.B. Zhang, J. Chen, L. Jin, W.L. Deng, J.F. Tang, H.T. Zhang, H. Pan, M.H. Zhu, W.Q. Yang, Z.L. Wang, *Adv. Mater.* 28 (2016) 1650–1656.
- [37] S.W. Chen, C.Z. Gao, W. Tang, H.R. Zhu, Y. Han, Q.W. Jiang, T. Li, X. Cao, Z.L. Wang, *Nanomater. Energy* 14 (2015) 217–225.
- [38] X.L. Cheng, B. Meng, X.S. Zhang, M.D. Han, Z.M. Su, H.X. Zhang, *Nanomater. Energy* 12 (2015) 19–25.
- [39] X.X. Chen, Y. Song, Z.M. Su, H.T. Chen, X.L. Cheng, J.X. Zhang, M.D. Han, H.X. Zhang, *Nanomater. Energy* 38 (2017) 43–50.
- [40] B. Meng, X.L. Cheng, X.S. Zhang, M.D. Han, W. Liu, H.X. Zhang, *Appl. Phys. Lett.* 104 (2014).
- [41] H. Chen, Y. Song, X. Cheng, H. Zhang, *Nano Energy* 56 (2019) 252–268.
- [42] X. Chen, L. Miao, H. Guo, H. Chen, Y. Song, Z. Su, H. Zhang, *Appl. Phys. Lett.* 112 (2018) 203902.
- [43] Q. Zheng, B. Shi, F. Fan, X. Wang, L. Yan, W. Yuan, S. Wang, H. Liu, Z. Li, Z.L. Wang, *Adv. Mater.* 26 (2014) 5851–5856.
- [44] S. Niu, Z.L. Wang, *Nanomater. Energy* 14 (2015) 161–192.
- [45] S.M. Niu, Y. Liu, Y.S. Zhou, S.H. Wang, L. Lin, Z.L. Wang, *Ieee T Electron Dev* 62 (2015) 641–647.
- [46] S. Niu, S. Wang, L. Lin, Y. Liu, Y.S. Zhou, Y. Hu, Z.L. Wang, *Energy Environ. Sci.* 6 (2013) 3576–3583.
- [47] S. Niu, Y. Liu, S. Wang, L. Lin, Y.S. Zhou, Y. Hu, Z.L. Wang, *Adv. Funct. Mater.* 24 (2014) 3332–3340.
- [48] S. Niu, Y. Liu, S. Wang, L. Lin, Y.S. Zhou, Y. Hu, Z.L. Wang, *Adv. Mater.* 25 (2013) 6184–6193.
- [49] S. Niu, Y. Liu, X. Chen, S. Wang, Y.S. Zhou, L. Lin, Y. Xie, Z.L. Wang, *Nanomater. Energy* 12 (2015) 760–774.
- [50] Y. Zi, S. Niu, J. Wang, Z. Wen, W. Tang, Z.L. Wang, *Nat. Commun.* 6 (2015) 8376.
- [51] G. Cheng, Z.H. Lin, L. Lin, Z.L. Du, Z.L. Wang, *ACS Nano* 7 (2013) 7383–7391.
- [52] X.L. Cheng, L.M. Miao, Y. Song, Z.M. Su, H.T. Chen, X.X. Chen, J.X. Zhang, H.X. Zhang, *Nanomater. Energy* 38 (2017) 448–456.
- [53] L. Xu, T.Z. Bu, X.D. Yang, C. Zhang, Z.L. Wang, *Nanomater. Energy* 49 (2018) 625–633.
- [54] L. Cheng, Q. Xu, Y.B. Zheng, X.F. Jia, Y. Qin, *Nat. Commun.* 9 (2018).
- [55] Y.L. Zi, J. Wang, S.H. Wang, S.M. Li, Z. Wen, H.Y. Guo, Z.L. Wang, *Nat. Commun.* 7 (2016).
- [56] A. Ghaffarnejad, J.Y. Hasani, R. Hinchet, Y. Lu, H. Zhang, A. Karami, D. Galayko, S.-W. Kim, P. Basset, *Nanomater. Energy* 51 (2018) 173–184.
- [57] H. Zhang, Y. Lu, A. Ghaffarnejad, P. Basset, *Nanomater. Energy* 51 (2018) 10–18.
- [58] G. Zhu, J. Chen, T.J. Zhang, Q.S. Jing, Z.L. Wang, *Nat. Commun.* 5 (2014).
- [59] X. Pu, M. Liu, L. Li, C. Zhang, Y. Pang, C. Jiang, L. Shao, W. Hu, Z.L. Wang, *Advanced Science* 3 (2016) 1500255.
- [60] Y.L. Zi, H.Y. Guo, J. Wang, Z. Wen, S.M. Li, C.G. Hu, Z.L. Wang, *Nanomater. Energy* 31 (2017) 302–310.
- [61] W. Tang, T. Zhou, C. Zhang, F.R. Fan, C.B. Han, Z.L. Wang, *Nanotechnology* 25 (2014).
- [62] S.M. Niu, X.F. Wang, F. Yi, Y.S. Zhou, Z.L. Wang, *Nat. Commun.* 6 (2015).
- [63] H. Qin, G. Cheng, Y. Zi, G. Gu, B. Zhang, W. Shang, F. Yang, J. Yang, Z. Du, Z.L. Wang, *Adv. Funct. Mater.* (2018) 1805216.
- [64] F.B. Xi, Y.K. Pang, W. Li, T. Jiang, L.M. Zhang, T. Guo, G.X. Liu, C. Zhang, Z.L. Wang, *Nanomater. Energy* 37 (2017) 168–176.
- [65] H. Chen, L. Miao, Z. Su, Y. Song, M. Han, X. Chen, X. Cheng, D. Chen, H. Zhang, *Nano Energy* 40 (2017) 65–72.
- [66] J.W. Campos, M. Beidaghi, K.B. Hatzell, C.R. Dennison, B. Musci, V. Presser, E.C. Kumbur, Y. Gogotsi, *Electrochim. Acta* 98 (2013) 123–130.
- [67] P. Simon, Y. Gogotsi, *Nat. Mater.* 7 (2008) 845–854.
- [68] J.R. Miller, P. Simon, *Science* 321 (2008) 651–652.
- [69] X.H. Lu, M.H. Yu, T. Zhai, G.M. Wang, S.L. Xie, T.Y. Liu, C.L. Liang, Y.X. Tong, Y. Li, *Nano Lett.* 13 (2013) 2628–2633.
- [70] Y.J. Kang, H. Chung, C.H. Han, W. Kim, *Nanotechnology* 23 (2012).
- [71] Z. Chen, J.W. To, C. Wang, Z. Lu, N. Liu, A. Chortos, L. Pan, F. Wei, Y. Cui, Z. Bao, *Advanced Energy Materials* 4 (2014) 1400207.
- [72] N. Li, Z. Chen, W. Ren, F. Li, H.-M. Cheng, *Proc. Natl. Acad. Sci. Unit. States Am.* 109 (2012) 17360–17365.
- [73] R. Li, Y. Wang, C. Zhou, C. Wang, X. Ba, Y. Li, X. Huang, J. Liu, *Adv. Funct. Mater.* 25 (2015) 5384–5394.
- [74] K.K. Fu, Y. Gong, J. Dai, A. Gong, X. Han, Y. Yao, C. Wang, Y. Wang, Y. Chen, C. Yan, *Proc. Natl. Acad. Sci. Unit. States Am.* 113 (2016) 7094–7099.
- [75] Y. Song, H. Chen, X. Chen, H. Wu, H. Guo, X. Cheng, B. Meng, H. Zhang, *Nano Energy* 53 (2018) 189–197.
- [76] Y. Song, H. Chen, Z. Su, X. Chen, L. Miao, J. Zhang, X. Cheng, H. Zhang, *Small* 13 (2017) 1702091.
- [77] Y. Song, X.-X. Chen, J.-X. Zhang, X.-L. Cheng, H.-X. Zhang, *J. Microelectromech. S* 26 (2017) 1055–1062.
- [78] X. Pu, L. Li, H. Song, C. Du, Z. Zhao, C. Jiang, G. Cao, W. Hu, Z.L. Wang, *Adv. Mater.* 27 (2015) 2472–2478.
- [79] Y. Song, J. Zhang, H. Guo, X. Chen, Z. Su, H. Chen, X. Cheng, H. Zhang, *Appl. Phys. Lett.* 111 (2017).
- [80] S.H. Wang, Z.H. Lin, S.M. Niu, L. Lin, Y.N. Xie, K.C. Pradel, Z.L. Wang, *ACS Nano* 7 (2013) 11263–11271.
- [81] X. Pu, M. Liu, L. Li, C. Zhang, Y. Pang, C. Jiang, L. Shao, W. Hu, Z.L. Wang, *Adv. Sci.* 3 (2016) 1500255.
- [82] X. Nan, C. Zhang, C. Liu, M. Liu, Z.L. Wang, G. Cao, *ACS Appl. Mater. Interfaces* 8 (2016) 862–870.
- [83] X. Liu, K. Zhao, Z.L. Wang, Y. Yang, *Advanced Energy Materials* 7 (2017).
- [84] T.T. Gao, K. Zhao, X. Liu, Y. Yang, *Nanomater. Energy* 41 (2017) 210–216.
- [85] F. Yi, J. Wang, X. Wang, S. Niu, S. Li, Q. Liao, Y. Xu, Z. You, Y. Zhang, Z.L. Wang, *ACS Nano* 10 (2016) 6519–6525.
- [86] X. Xiao, T.Q. Li, P.H. Yang, Y. Gao, H.Y. Jin, W.J. Ni, W.H. Zhan, X.H. Zhang, Y.Z. Cao, J.W. Zhong, L. Gong, W.C. Yen, W.J. Mai, J. Chen, K.F. Huo, Y.L. Chueh, Z.L. Wang, J. Zhou, *ACS Nano* 6 (2012) 9200–9206.
- [87] J. Wang, Z. Wen, Y. Zi, P. Zhou, J. Lin, H. Guo, Y. Xu, Z.L. Wang, *Adv. Funct. Mater.* 26 (2016) 1070–1076.
- [88] H. Guo, M.H. Yeh, Y. Zi, Z. Wen, J. Chen, G. Liu, C. Hu, Z.L. Wang, *ACS Nano* 11 (2017) 4475–4482.
- [89] H. Guo, M.H. Yeh, Y.C. Lai, Y. Zi, C. Wu, Z. Wen, C. Hu, Z.L. Wang, *ACS Nano* 10 (2016) 10580–10588.
- [90] K. Dong, Y.C. Wang, J. Deng, Y. Dai, S.L. Zhang, H. Zou, B. Gu, B. Sun, Z.L. Wang, *ACS Nano* 11 (2017) 9490–9499.
- [91] Y. Song, X. Cheng, H. Chen, J. Huang, X. Chen, M. Han, Z. Su, B. Meng, Z. Song, H. Zhang, *J. Mater. Chem.* 4 (2016) 14298–14306.
- [92] G. Zhu, Z.H. Lin, Q.S. Jing, P. Bai, C.F. Pan, Y. Yang, Y.S. Zhou, Z.L. Wang, *Nano Lett.* 13 (2013) 847–853.
- [93] B. Meng, W. Tang, Z.H. Too, X.S. Zhang, M.D. Han, W. Liu, H.X. Zhang, *Energy Environ. Sci.* 6 (2013) 3235–3240.
- [94] S. Wang, Y. Xie, S. Niu, L. Lin, Z.L. Wang, *Adv. Mater.* 26 (2014) 2818–2824.
- [95] T. Jiang, X. Chen, C.B. Han, W. Tang, Z.L. Wang, *Adv. Funct. Mater.* 25 (2015) 2928–2938.
- [96] S. Niu, S. Wang, Y. Liu, Y.S. Zhou, L. Lin, Y. Hu, K.C. Pradel, Z.L. Wang, *Energy Environ. Sci.* 7 (2014) 2339–2349.
- [97] S.M. Niu, Z.L. Wang, *Nanomater. Energy* 14 (2015) 161–192.
- [98] G. Cheng, H. Zheng, F. Yang, L. Zhao, M. Zheng, J. Yang, H. Qin, Z. Du, Z.L. Wang, *Nanomater. Energy* 44 (2018) 208–216.
- [99] J. Yang, F. Yang, L. Zhao, W. Shang, H. Qin, S. Wang, X. Jiang, G. Cheng, Z. Du, *Nanomater. Energy* 46 (2018) 220–228.
- [100] A. Ghaffarnejad, Y. Lu, R. Hinchet, D. Galayko, J.Y. Hasani, S.W. Kim, P. Basset, *Electron. Lett.* 54 (2018) 378–379.
- [101] C.B. Han, C. Zhang, W. Tang, X.H. Li, Z.L. Wang, *Nano Res* 8 (2015) 722–730.
- [102] D. Bhatia, J. Lee, H.J. Hwang, J.M. Baik, S. Kim, D. Choi, *Advanced Energy Materials* 8 (2018).
- [103] H. Guo, Z. Wen, Y. Zi, M.H. Yeh, J. Wang, L. Zhu, C. Hu, Z.L. Wang, *Advanced Energy Materials* 6 (2016) 1501593.
- [104] S. Wang, X. Mu, Y. Yang, C. Sun, A.Y. Gu, Z.L. Wang, *Adv. Mater.* 27 (2015) 240–248.
- [105] X.D. Zhong, Y. Yang, X. Wang, Z.L. Wang, *Nanomater. Energy* 13 (2015) 771–780.
- [106] S. Boisseau, G. Despesse, S. Monfray, O. Puscasu, T. Skotnicki, *Smart Mater. Struct.* 22 (2013).
- [107] Y. Song, H. Wang, X. Cheng, G. Li, X. Chen, H. Chen, L. Miao, X. Zhang, H. Zhang, *Nano Energy* 55 (2019) 29–36.
- [108] I. Park, J. Maeng, D. Lim, M. Shim, J. Jeong, C. Kim, *Solid-State Circuits Conference-(ISSCC), IEEE International*, 2018, pp. 146–148 IEEE2018.
- [109] J.J. Yang, F. Yang, L. Zhao, W.Y. Shang, H.F. Qin, S.J. Wang, X.H. Jiang, G. Cheng, Z.L. Du, *Nanomater. Energy* 46 (2018) 220–228.
- [110] Z.L. Wang, G. Zhu, Y. Yang, S.H. Wang, C.F. Pan, *Mater. Today* 15 (2012) 532–543.

- [111] X.S. Zhang, M.D. Han, B. Kim, J.F. Bao, J. Brugger, H.X. Zhang, *Nano Energy* 47 (2018) 410–426.
- [112] H.D. Hou, Q.K. Xu, Y.K. Pang, L. Li, J.L. Wang, C. Zhang, C.W. Sun, *Advanced Science* 4 (2017).
- [113] P. Poizot, S. Laruelle, S. Grugeon, L. Dupont, J. Tarascon, *Nature* 407 (2000) 496.
- [114] M. Han, X.-S. Zhang, B. Meng, W. Liu, W. Tang, X. Sun, W. Wang, H. Zhang, *ACS Nano* 7 (2013) 8554–8560.
- [115] Y. Yang, H. Zhang, G. Zhu, S. Lee, Z.-H. Lin, Z.L. Wang, *ACS Nano* 7 (2012) 785–790.
- [116] Y. Guo, X.-S. Zhang, Y. Wang, W. Gong, Q. Zhang, H. Wang, J. Brugger, *Nano Energy* 48 (2018) 152–160.
- [117] J.H. Lee, K.Y. Lee, M.K. Gupta, T.Y. Kim, D.Y. Lee, J. Oh, C. Ryu, W.J. Yoo, C.Y. Kang, S.J. Yoon, *Adv. Mater.* 26 (2014) 765–769.
- [118] X. Chen, H. Guo, H. Wu, H. Chen, Y. Song, Z. Su, H.J. Zhang, *Nano Energy* 49 (2018) 51–58.
- [119] X. Chen, M. Han, H. Chen, X. Cheng, Y. Song, Z. Su, Y. Jiang, H. Zhang, *Nanoscale* 9 (2017) 1263–1270.
- [120] Y. Zi, L. Lin, J. Wang, S. Wang, J. Chen, X. Fan, P.K. Yang, F. Yi, Z.L. Wang, *Adv. mater.* 27 (2015) 2340–2347.
- [121] Y. Yang, Z.L. Wang, *Nano Energy* 14 (2015) 245–256.
- [122] M. Han, X. Chen, B. Yu, H.J. Zhang, *Adv. Electron. Mater.* 1 (2015) 1500187.



Xiao-Liang Cheng received the B.S. degree from the University of Electronic Science and Technology of China, Chengdu, in 2014. He is currently pursuing the Ph.D. degree at the National Key Laboratory of Nano/Micro Fabrication Technology, Peking University, Beijing, China. His research interests mainly include design and fabrication of nanogenerator and mechanical energy harvester.



In 2006, she received the National Invention Award of Science and Technology.

Hai-Xia (Alice) Zhang (SM'10) received the Ph.D. degree in mechanical engineering from Huazhong University of Science and Technology, Wuhan, China, 1998. She is currently a Professor with the Institute of Microelectronics, Peking University, Beijing, China. She joined the faculty of the Institute of Microelectronics in 2001 after finishing her post-doctoral research in Tsinghua University. Her research interests include MEMS design and fabrication technology, SiC MEMS, and micro energy technology. She has served on the General Chair of the IEEE NEMS 2013 Conference, the Organizing Chair of Transducers'11. As the Founder of the International Contest of Applications in Network of things, she has been organizing this world-wide event since 2007.



His research on self-powered nanosystems has inspired the worldwide effort in academia and industry for studying energy for micro-nano-systems, which is now a distinct disciplinary in energy research and future sensor networks. He coined and pioneered the field of piezotronics and piezo-phototronics by introducing piezoelectric potential gated charge transport process in fabricating new electronic and optoelectronic devices.

Zhong Lin (ZL) Wang received his Ph.D. from Arizona State University in physics. He now is the Hightower Chair in Materials Science and Engineering, Regents' Professor, Engineering Distinguished Professor and Director, Center for Nanostructure Characterization, at Georgia Tech. Dr. Wang has made original and innovative contributions to the synthesis, discovery, characterization and understanding of fundamental physical properties of oxide nanobelts and nanowires, as well as applications of nanowires in energy sciences, electronics, optoelectronics and biological science. His discovery and breakthroughs in developing nanogenerators established the principle and technological road map for harvesting mechanical energy from environment and biological systems for powering personal electronics.